Current Topics in Peptide & Protein Research
Vol. 22, 2021

Original Article

Estimation of hydrophobicity of segments in Amyloid β42 partly comprising D-amino acids

Toratane Munegumi*

Department of Science Education, Naruto University of Education, 748 Nakashima, Takashima, Naruto-Cho, Naruto, Tokushima 772-8502, Japan.

ABSTRACT

Terrestrial D-amino acids have been found as either free amino acids or the components of peptides and proteins. The proteins originally comprising L-amino acids sometimes change into the D-amino acid-comprising form following natural epimerization. The resulting peptides and proteins have different physical, chemical, and/or biological properties from the original forms. Looking at the oligopeptide region of proteins, the hydrophobicity of oligopeptides has been calculated using semiempirical methods. The oligopeptides partly comprising D-amino acids mostly have more hydrophobic regions than the oligopeptides comprising only L-amino acids. This research focuses on the epimerization and isomerization of aspartic acid residues of the segments in the wild type and Italian mutant of Amyloid β42 to estimate the relationship between the epimerization and the hydrophobicity change. Higher hydrophobicity is known to facilitate the aggregation and toxicity of Amyloid β42 and its mutants. This research used a linear relationship between experimental log *P* and calculated log *P* (Clog *P*) in which log *P* is the logarithm of the partition coefficient *P* in 1-octanol to water. The calculation using semiempirical methods (PM5) validated the relationship between the structure change and the hydrophobicity during the epimerization of the oligopeptides. The epimerization at the two common aspartic residues, D^1 and D^7 for the wild type and the Italian mutant, gave smaller Clog *P* values than non-epimerized ones. The epimerization at another common residue D^{23} showed larger Clog *P* for the hexapeptide segments. Clog *P* values of the epimerized hexapeptide segments of the Italian mutant were larger than those of the wild type. The results suggest that the original and D-epimer at D^{23} of the Italian mutant must be more hydrophobic than those of the wild type. The estimation agrees with the experimental results of aggregation.

KEYWORDS: amino acids, oligopeptide, heterochiral, homochiral, partition coefficient, epimerization.

INTRODUCTION

Sequences comprising D-amino acid residues [1-4] have been found in peptide antibiotics [2-4], peptide glycan [2-4], bioactive peptides [4-14], and human tissues [3, 14-24]. Proteins are originally made from L-amino acids coded on deoxyribonucleic acid. Some types of L-amino acid residues in such proteins can sometimes become D-amino acid residues by epimerization [16, 20, 25, 26], which is a type of isomerization reaction to yield diastereomers. The emergence of D-aspartic acid residues by epimerization has been found in proteins [1-4] such as myelin [7], myelin basic proteins [7], Amyloid β [17], aging of human lens αA-crystallin [19-21], and others [1-4]. Aspartic acid racemizes as the free form [27] and epimerizes as amino acid residues in the

*Email id: tmunegumi@naruto-u.ac.jp

peptide form [28] with the fastest rate constants of all the amino acids. Aspartic acid has an inductive side chain, a methyl carboxy group, which also can remove α-hydrogen from aspartic acid or its residue [27] through an achiral intermediate to racemize or epimerize. However, β-DL-aspartyl residues have been detected in αA-crystallin [20, 29]. From the results, imide intermediates were suggested [29-32] as shown in Figure 1.

Each L-aspartic acid residue in peptides and proteins generally has a side-chain group, methyl carboxy that can intramolecularly dehydrate and cyclize to an L-imide. The resulting L-imide structure can give an L-aspartic acid residue (L-Asp), an L-β-aspartic residue (L-βAsp), or an achiral cyclic structure, which can isomerize to D-imide. These reaction paths are categorized as a type of epimerization in peptides and proteins. D-imide can react again to lead to a D-aspartic acid residue (D-Asp), a D-β-aspartic residue (D-βAsp), or reverse to the achiral cyclic structure. After the set of reactions, six types of isomers may be found as shown in Figure 1.

These epimerized proteins resulting in D-amino acid residues may be able to make the conformation of the proteins more hydrophobic. Previous studies [25, 26] have demonstrated that the emergence of D-amino acid residues in oligopeptides and proteins will usually lead to a segmental decrease in water solubility of the corresponding area. The water solubility of a compound increases with increasing hydrophilicity and decreases with increasing hydrophobicity. Several research results [33-38] have shown the differences in the hydrophobicity between the oligopeptides (homochiral peptide diastereomers) composed of only L-amino acids and the oligopeptides (heterochiral peptide diastereomers) comprising D-amino acids.

The previous reports [25, 26] have clarified that most of the oligopeptides partly comprising D-amino acid residues are usually more hydrophobic than the oligopeptides composed of all L-amino acid residues. Reverse-phase high-performance liquid chromatography (RP-HPLC) has been used for the separation of oligopeptide diastereomers to demonstrate that many heterochiral peptide

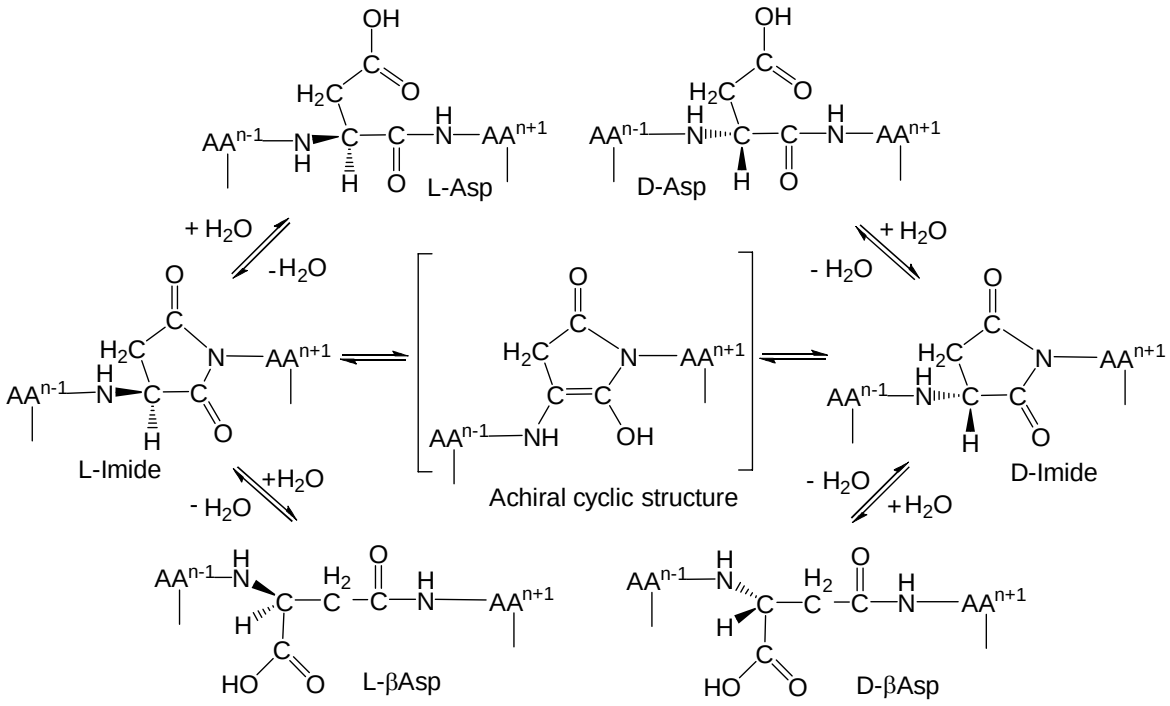

Figure 1. Epimerization mechanism facilitated by the imide structure formation from aspartyl residue (AA^n) in peptides. AA^{n-1} and AA^{n+1} are the *N*-terminal side and *C*-terminal side residues of the AA^n residue.

diastereomers are eluted later than their homochiral peptide diastereomers on RP-HPLC. Analyses on RP-HPLC can be used to determine the coefficients *a*, *b* in Eqn. 1. The capacity factor k' is the ratio of the retention time difference ($t_R - t_0$) to the retention time (t_0) of a nonretarded compound in RP-HPLC: $k' = (t_R - t_0)/t_0$. The log *P* [39-48] values, namely, the logarithm of an experimental partition coefficient *P* for 1-octanol in water to be an indicator of hydrophobicity, can be used for a hydrophobicity scale of peptides. There is a relationship between the log *P* value and the capacity factor (k') on RP-HPLC as shown in Eqn. 1 [48, 49].

$$\log P = a \log k' + b \quad (1)$$

The log *P* values have been calculated with a semiempirical method using a computer program for evaluating the hydrophobicity. The log *P* values (Clog *P*) [46, 50] calculated by a semiempirical method using a computer program can evaluate the hydrophobicity change of peptides in the epimerized amino acid residues in many peptides and proteins [25, 26].

Amyloid β40 and β42 are known to be the main components of amyloid fibrils, which are suggested to have neurotoxicity related to Alzheimer's disease [51, 52]. Several types of mutants of the amyloids shown in Figure 2 have been found [51].

The wild types of Amyloid β40 and β42 have common sequences from the *N*-terminal to the 40th amino acid residue from the *N*-terminus. The amino acid residues of AA^{21}, AA^{22}, and AA^{23} are Ala (A), Glu (E), and Asp (D), respectively. The *C*-terminal residue, AA^{41}-AA^{42} ($I^{41}A^{42}$), contributes to producing the higher aggregation rate of Amyloid β42 than Amyloid β40 [51, 53]. The fastest aggregation rate was detected in an experiment using the Italian mutant comprising A^{21}, K^{22}, and D^{23}. The Italian mutant is suggested as the most hydrophobic of the peptides shown in Figure 2.

The reason for the highest aggregation rate of the Italian mutant was explained by the highest hydrophobicity derived from the stability of the β-sheet structure [51]. Basically, Amyloid β42 has two turn structures in two different places: (1) E^{22}-D^{23} and (2) G^{38}-G^{39}. The back-and-forth character of each turn structure induces each β-sheet pairing to be more hydrophobic and aggregate between different Amyloid β42 molecules [51, 53]. The β-sheet pairing in the back-and-forth changes of G^{38}-G^{39} can be induced by the conformation change of I^{41} along with changing the trans peptide bond to cis [51, 53]. However, the feature of the β-sheet pairing involving the AA^{22}-AA^{23} turn structure of mutants may depend on the sequences in AA^{22}-AA^{23}. The Italian mutant is the

$D^1AEFRHD^7SGY^{10}$ $E^{11}VHHQKLVFF^{20}$ $AA^{21}AA^{22}AA^{23}$ $V^{24}G^{25}SNKGA^{30}$ $I^{31}IGLMVGGVV^{40}$ $I^{41}A^{42}$

Amyloid β40 and β42 mutation type	AA^{21}	AA^{22}	AA^{23}
Wild	A	E	D
Flemish	G	E	D
Arctic	A	G	D
Dutch	A	Q	D
Italian	A	K	D
Iowa	A	E	N

Figure 2. Peptide sequences of the wild and mutant types of Amyloid β40 and β42.

most hydrophobic in the amyloids including mutants and the wild type. The reason has been explained by the ion bonding between the side-chain ammonium cation of K^{22} and the side-chain carboxy anion of D^{23} [51].

The epimerization in aspartic residues D^1, D^7, and D^{23} as a different factor has been dealt with for the increase in the hydrophobicity of Amyloids β40 and β42 [52-57]. Tryptic digestions [52] of the wild type of Amyloid β42 revealed epimerization at D^1 and D^7 but not at D^{23}. The epimerization was explained by the reaction mechanism through imide formation at the aspartic residues. The L-imide structure can more easily release a proton than usual L-aspartic residues to give an achiral cyclic structure, which can change to D-imide and then D-aspartic residues in the epimerization mechanism shown in Figure 2. The lack of isomerization and epimerization at D^{23} was explained by limiting imide formation with V^{24} because of its bulky hydrophobic side chain. These results of epimerization at D (Asp) residues have not been discussed as depending on the hydrophobicity change of Amyloid β.

Other researchers treated the synthesized Amyloid β42 analogues comprising D-aspartic residues to compare their hydrophobicity [54-56]. Fibril formation was enhanced using Amyloid β42 analogues modified with D-Asp at D^7 or D^{23} but not D^1 of the wild type [54]. Research [57] using other analogues that switched D^{23} to the isomers —L-isoAsp (L-βAsp), D-Asp, and D-isoAsp (D-βAsp)— reported that L-βAsp and D-Asp showed a similar aggregative ability to the wild type and D-βAsp showed weak aggregative ability. Further, simultaneously switching both D^7 and D^{23} to D-Asp [55] enhanced oligomerization, fibril formation, and neurotoxic effect compared with the wild type but switching D^1, D^7, and D^{23} to D-Asp suppressed malignant effects.

Although there are only three Asp residues in Amyloid β42, double or triple epimerization forms many types of analogues. The relationship between epimerization and aggregation may need many types of peptide syntheses. However, a calculation without synthesis can simulate many types of analogues. This paper reports the differences between the segmental sequences in Amyloid β42 composed of L-amino acids and the same sequences comprising a D-Asp residue in Clog *P* values. The research focuses on the epimerization at the common residues (D^1, D^7 and D^{23}) between the wild type and Italian mutant of Amyloid β42 to compare the values of Clog *P* as a convenient factor for measuring hydrophobicity.

MATERIALS AND METHODS

The mechanically optimum structures of the diastereomeric peptides were determined by calculation using molecular mechanics (MM3) from the SCIGRESS program from Fujitsu, Tokyo, Japan. Subsequently, a semiempirical calculation for the resulting optimum structure was carried out using Molecular Orbital Package (MOPAC) based on the PM5 Hamiltonian [41] to give the heat of formation in vacuum and in water. The energy unit used was kcal/mol (1 kJ/mol = 4.18 kcal/mol). The solvent-accessible surface area for the stable structures was calculated and expressed in square Ångstrom (1.0 $Å^2$ = 0.01 nm^2). The Clog *P* value for the peptide structures was sequentially calculated on a spreadsheet, an attachment program to SCIGRESS.

For estimating actual log *P* values, the relationship between Clog *P* and experimental log *P* (Exptl. log P) values of amino acids and oligopeptides was evaluated. Exptl. log *P* values have been correlated to their log *k*′ values reported in the literature [26]. The present research corrected the correlation using the previously reported log *P* values [39, 40] of amino acids and peptides and log *k*′. A semiempirical program based on MOPAC with the PM5 Hamiltonian was used for the calculation. Clog *P* values using the PM5 method can be determined from the formula shown in Eqn. 2.

$$\text{Clog } P = -0.0305\,(A) + 0.0215\,(B) + 0.0266\,(C) - 1.2673\,\text{sqrt}\,(D) - 3.5427\,\text{sqrt}\,(E) + 1.8021 \quad (2)$$

This equation was obtained by a comparison of Exptl. log *P* for many types of amino acids and *N*-acetyl peptide amides [46] with those of Clog *P* values. The factors for the five functions (A to E) were estimated and optimized to produce the most efficient linear correlation between Exptl. log *P* and Clog *P* values. In this equation, Clog *P* is composed of several functions as follows: A: heat of formation (kcal/mol) at the PM5 geometry, B: solvent-accessible surface area (square Ångstroms),

C: the heat of formation in water at the PM5 geometry, D: number of nitrogen atoms in the molecule, E: number of oxygen atoms in the molecule.

RESULTS AND DISCUSSION

1. Estimation of experimental log *P* values by calculated log *P*

Exptl. log *P* and Clog *P* values of amino acids and *N*-acetyl peptide amides (Ac-peptide amides) are listed in Table 1.

A linear correlation has been reported [25, 26] between Exptl. log *P* and Clog *P* of amino acids. Ac-peptide amides were used for the model compounds estimating log *P* values of peptide sequences of Amyloid β42. These two types of compounds are useful for estimating log *P* values in the log *P* range between about –5 and 1. The data in Table 1 are plotted in Figure 3, which reveals a good linear relationship (R^2 = 0.978) between Exptl. log *P* and Clog *P* values. The relationship can be used for predicting the actual Exptl. log *P* values of the restricted Amyloid β42 sequences from Clog *P* values.

2. Estimation of log *P* values of segmental Amyloid β42 including D^1

The Clog *P* of the segment sequence $D^1A^2E^3F^4$ was calculated as Asp-Ala-Glu-Phe-NH_2, which has a *C*-terminal amide structure. Calculated values of Clog *P* for the segmental Amyloid β42 including D^1 are shown in Table 2 and Figure 4. Clog *P* values were in the range –3.51 to –1.39. Smaller Clog *P* values of epimers were obtained in most D-epimers more than L-epimers except for D19 and D110. For example, the Clog *P* value for D12 (D-form, –2.32) was smaller than for D11 (L-form, –1.92). The epimerization in D^1 will produce more hydrophilic structures.

3. Estimation of log *P* values of segmental Amyloid β42 including D^7

The Clog *P* of the segment sequence $H^6D^7S^8G^9Y^{10}$ was calculated as Ac-His-Asp-Ser-Gly-Tyr-NH_2, which has a *C*-terminal amide structure. Calculated values of Clog *P* for segmental Amyloid β42 including D^7 are shown in Table 3 and Figure 5. Smaller Clog *P* values were obtained in all D-epimers more than L-epimers. The epimerization at D^7 will form more hydrophilic structures. The peptide structures including Histidine residues are according to the structures in basic solutions (pH 8 to 9), in which the side chain of Tyr almost does not ionize. The peptide structures including the HisH sequence are neutral or acidic (pH < 7). The peptide structures including both HisH and AspH (or βAspH) are according to acidic conditions (pH < 2). Therefore, at pH lower than 9, the peptide sequences having the D-form at D^7 are more hydrophilic than those of the original sequences having the L-form. The hydrophilicity of segment peptides isomerized at D^1 means lower aggregation, which fits with the results having actual lower aggregation features. As shown above [52-57], Amyloid β42 in which both D^7 and D^{23} were exchanged to D-Asp enhanced fibril formation. Therefore, the epimerization at D^{23} may contribute to more hydrophobicity of Amyloid β42 even though the epimerization at D^7 makes hydrophilicity.

4. Estimation of log *P* values of segmental Amyloid β42 including D^{23}

4.1. Chemical structures of segmental Amyloid β42 including D^{23}

As shown in Figure 2, there are several mutants of Amyloid β42. The Italian mutant is the most hydrophobic and the most easily aggregated among them. The following sections compare Clog *P* of the wild type of segment peptides and epimerized peptides with those of the Italian mutant. Figure 6 shows the chemical structures of the bending segmental areas (AA^{21}-AA^{22}-AA^{23}-AA^{24}) of the wild type (A^{21}-E^{22}-D^{23}-V^{24}) and the Italian mutant (A^{21}-K^{22}-D^{23}-V^{24}) of Amyloid β42. The bending segmental area of peptides can be classified into three types of segments: α-peptides, imides, and β-peptides. Each type of segment has two features, namely L-Asp or D-Asp at D^{23} and trans 1 or trans 2. Because of the interactions between the two side chains of AA^{22} and AA^{23}, the bending at this sequence site may be more stable. There may be a substantial barrier against the conformation change between trans 1 and trans 2. This research presumes that both trans 1 and trans 2 are not tautomerized but stabilized. The interactions between the side chains of AA^{22}

Table 1. Calculated log *P* values of amino acids and *N*-acetyl-peptide amides.

Amino acids and *N*-Acetyl-Peptide amides	**A: Hf in vacuum (kcal/mol)**	**B: Solvent accessible area ($Å^2$)**	**C: Hf in H_2O (kcal/mol)**	**D: Number of N atom**	**E: Number of O atom**	**Clog P**	**Exptl. log P**
Glycine (Gly)	-80.70	105.5	-133.1	1	2	-3.30	-3.21
Alanine (Ala)	-88.10	123.5	-138.4	1	2	-2.82	-2.85
Valine (Val)	-99.50	152.9	-144.9	1	2	-2.02	-2.26
Leucine (Leu)	-106.7	175.1	-153.1	1	2	-1.54	-1.74
Isoleucine (Ile)	-104.1	172.7	-148.3	1	2	-1.54	-1.76
Serine (Ser)	-133.0	133.3	-179.2	1	3	-3.46	-3.33
Threonine (Thr)	-140.7	149.3	-183.0	1	3	-2.98	-2.98
Phenylalanine (Phe)	-68.40	197.6	-114.8	1	2	-1.21	-1.52
Tyrosine (Tyr)	-112.3	207.8	-162.9	1	3	-2.06	-2.66
Tryptophane (Trp)	-47.10	226.2	-95.0	2	2	-1.24	-1.06
Proline (Pro)	-86.30	146.8	-130.6	1	2	-2.17	-2.54
Methionine (Met)	-89.60	184.9	-139.5	1	2	-1.49	-2.00
Glutamine (Gln)	-147.1	178.8	-199.2	2	3	-3.11	-3.15
Asparagine (Arg)	-142.1	157.9	-189.5	2	3	-3.45	-3.82
Glutamic acid (GluH)	-183.4	175.0	-238.2	1	4	-3.55	-3.66
Glutamic $acid^-$ (Glu^-)	-263.3	170.6	-348.9	1	4	-4.15	-3.66
Aspartic acid (AspH)	-183.1	154.6	-229.6	1	4	-3.77	-3.68
Aspartic $acid^-$ (Asp^-)	-254.4	151.4	-344.5	1	4	-4.72	-3.68
$ArginineH^+$	39.0	222.0	-45.7	4	2	-3.39	-4.20
$LysineH^+$	41.2	198.0	-36.5	2	2	-2.98	-3.05
His	-56.6	182.0	-106.9	3	2	-2.62	-2.52
Ac-Tyr-Phe-NH_2	-152.6	375.8	-183.9	3	4	0.35	0.54
Ac-Thr-Val-NH_2	-217.0	289.1	-242.8	3	4	-1.12	-1.25
Ac-Ala-Leu-NH_2	-174.6	279.8	-197.9	3	3	-0.47	-0.54
Ac-Trp-Val-NH_2	-121.6	363.4	-149.7	4	3	0.65	0.73
Ac-Ser-Val-NH_2	-207.9	277.4	-235.0	3	4	-1.44	-1.53
Ac-Val-Gly-NH_2	-160.5	246.8	-185.2	3	3	-1.27	0.45
Ac-Trp-Gly-Phe-NH_2	-130.3	439.4	-166.3	5	4	0.86	0.99
Ac-Leu-Thr-Leu-NH_2	-288.1	414.3	-317.9	4	5	0.56	0.24
Ac-Leu-Ser-Phe-NH_2	-239.0	418.6	-270.5	4	5	0.42	0.23
Ac-Ala-Tyr-Leu-NH_2	-241.2	409.8	-274.8	4	5	0.18	-0.04

Hf: Heat of formation; Clog P: Calculated log P; Exptl. Log P: Experimental log P.
Glutamic $acid^-$ (Glu^-) and Aspartic $acid^-$ (Asp^-): side chains are carboxylate.
Glutamic acid (GluH) and Aspartic acid (AspH): side chains are protonated; Ac: Acetyl-.

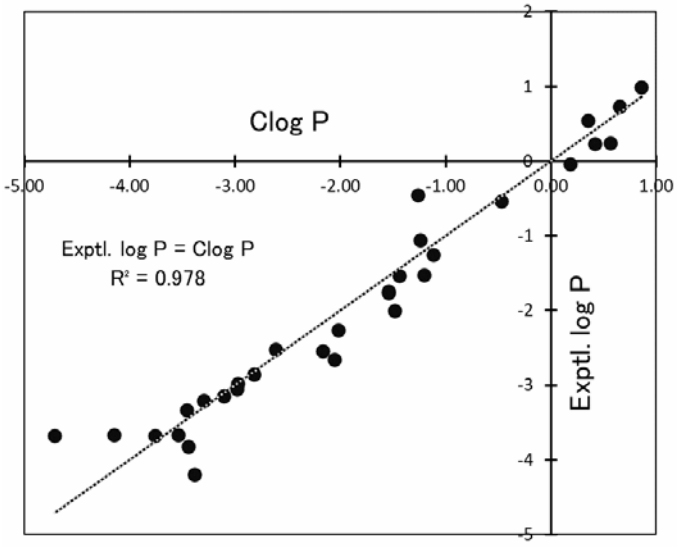

Figure 3. The linear relationship between Experimental log *P* and Clog *P*.
Clog *P* values were calculated by inserting values of **A:** ΔH_f in vacuum (kcal/mol); **B:** Solvent accessible area (Å^2); **C:** ΔH_f in H_2O (kcal/mol); **D:** Number of N atoms; and **E:** Number of O atoms into the equation: Clog *P* = –0.0305 (A) + 0.0215 (B) + 0.0266 (C) – 1.2673 sqrt (D) – 3.5427 sqrt (E) + 1.8021.

Table 2. Calculated log *P* values of sequences from D[1] to F[4] in Amyloid β42 including those isomerized at D[1].

No.	Peptide amides	A: Hf in vacuum (kcal/mol)	B: Solvent accessible area (Å^2)	C: Hf in H_2O (kcal/mol)	D: Number of N atom	E: Number of O atom	Clog P
D11	Asp-Ala-Glu-Phe-NH_2	-438.9	450.9	-524.4	5	8	-1.92
D12	D-Asp-Ala-Glu-Phe-NH_2	-440.7	437.6	-530.7	5	8	-2.32
D13	AspH-Ala-GluH-Phe-NH_2	-216.1	486.5	-319.0	5	8	-2.49
D14	D-AspH-Ala-GluH-Phe-NH_2	-222.1	465.2	-317.3	5	8	-2.72
D15	Aspimide-Ala-Glu-Phe-NH_2	-309.3	424.6	-358.7	5	7	-1.39
D16	D-Aspimide-Ala-Glu-Phe-NH_2	-312.4	410.3	-359.5	5	7	-1.59
D17	Aspimide-Ala-GluH-Phe-NH_2	-152.3	463.6	-259.2	5	7	-2.69
D18	D-Aspimide-Ala-GluH-Phe-NH_2	-160.5	404.2	-251.7	5	7	-3.51
D19	βAsp-Ala-Glu-Phe-NH_2	-444.8	428.0	-535.4	5	8	-2.53
D110	D-βAsp-Ala-Glu-Phe-NH_2	-445.9	435.3	-539.8	5	8	-2.45
D111	βAspH-Ala-GluH-Phe-NH_2	-222.8	456.6	-310.8	5	8	-2.71
D112	D-βAspH-Ala-GluH-Phe-NH_2	-227.5	450.5	-312.9	5	8	-2.75

Hf: Heat of formation; Clog P: Calculated log P.
Glutamic acid (Glu) and Aspartic acid (Asp): side chains are carboxylate.
Glutamic acid (GluH) and Aspartic acid (AspH): side chains are protonated.
All the amino acids without heading D- have L-chirality.; Aspimide has an imide structure.
Heading only β is β-carboxy of L-Asp making peptide bond with Ala residue.
Heading D-β is β-carboxy of D-Asp making peptide bond with Ala residue.

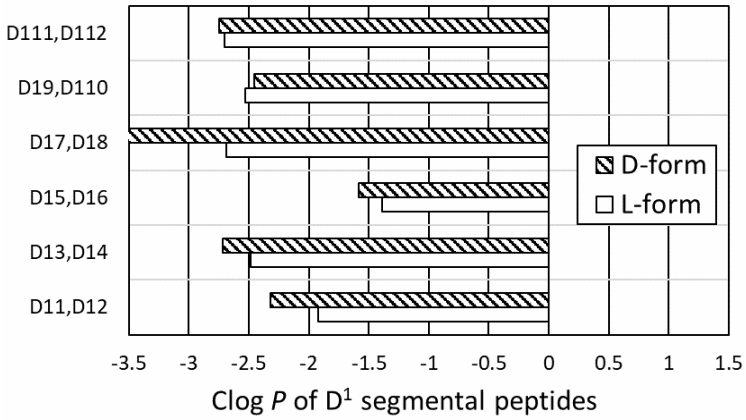

Figure 4. Comparison of Clog *P* values between the L-epimer and D-epimer of the sequences including isomerized Asp residues from D^1 to F^4 in Amyloid β42.

Table 3. Calculated log *P* values of sequences $H^6D^7S^8G^9Y^{10}$ in Amyloid β42 including those isomerized at D^7.

No.	*N*-Acetyl-Peptide amides	A: Hf in vacuum (kcal/mol)	B: Solvent accessible area (Å^2)	C: Hf in H_2O (kcal/mol)	D: Number of N atom	E: Number of O atom	Clog P
D71	Ac-His-Asp-Ser-Gly-Tyr-NH_2	-480.9	549.7	-572.4	8	10	-1.73
D72	Ac-His-D-Asp-Ser-Gly-Tyr-NH_2	-479.7	555.8	-585.9	8	10	-1.99
D73	Ac-HisH-Asp-Ser-Gly-Tyr-NH_2	-410.6	567.7	-477.6	8	10	-0.96
D74	Ac-HisH-D-Asp-Ser-Gly-Tyr-NH_2	-407.1	539.1	-481.4	8	10	-1.78
D75	Ac-HisH-AspH-Ser-Gly-Tyr-NH_2	-269.9	549.9	-369.5	8	10	-2.76
D76	Ac-HisH-D-AspH-Ser-Gly-Tyr-NH_2	-274.0	534.2	-368.8	8	10	-2.95
D77	Ac-His-Aspimide-Ser-Gly-Tyr-NH_2	-350.7	567.3	-412.5	8	9	-0.49
D78	Ac-His-D-Aspimide-Ser-Gly-Tyr-NH_2	-350.0	548.0	-408.9	8	9	-0.83
D79	Ac-HisH-Aspimide-Ser-Gly-Tyr-NH_2	-207.3	564.2	-310.2	8	9	-2.21
D710	Ac-HisH-D-Aspimide-Ser-Gly-Tyr-NH_2	-212.6	545.8	-306.4	8	9	-2.34
D711	Ac-His-β-Asp-Ser-Gly-Tyr-NH_2	-482.8	559.0	-585.5	8	10	-1.82
D712	Ac-His-Dβ-Asp-Ser-Gly-Tyr-NH_2	-481.3	550.8	-581.3	8	10	-1.93
D713	Ac-HisH-β-Asp-Ser-Gly-Tyr-NH_2	-388.6	568.8	-476.0	8	10	-1.57
D714	Ac-HisH-Dβ-Asp-Ser-Gly-Tyr-NH_2	-386.9	547.8	-474.8	8	10	-2.04
D715	Ac-HisH-β-AspH-Ser-Gly-Tyr-NH_2	-273.1	567.5	-373.9	8	10	-2.40
D716	Ac-HisH-Dβ-AspH-Ser-Gly-Tyr-NH_2	-273.9	562.5	-370.8	8	10	-2.40

Hf: Heat of formation; Clog P: Calculated log P.
Histidine (HisH) and Aspartic acid (AspH): side chains are protonated.
All the amino acids without heading D- have L-chirality.; Aspimide has an imide structure.
Heading only β is β-carboxy of L-Asp making peptide bond with Ala residue.
Heading D-β is β-carboxy of D-Asp making peptide bond with Ala residue.

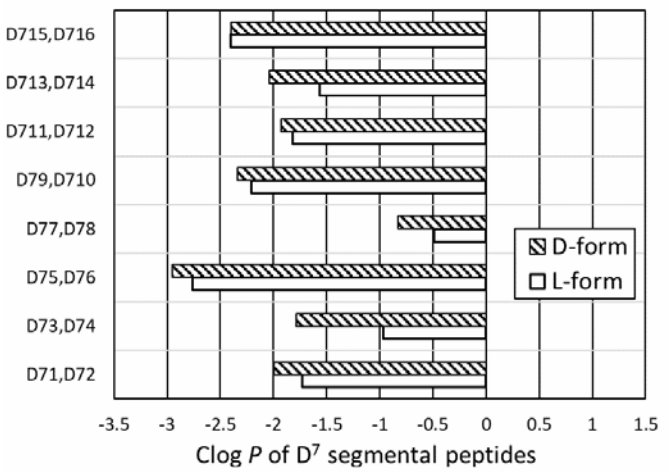

Figure 5. Comparison of Clog *P* values between the L-epimer and D-epimer of the sequences H^6D^7 to Y^{10} including isomerized Asp residues in Amyloid β42.

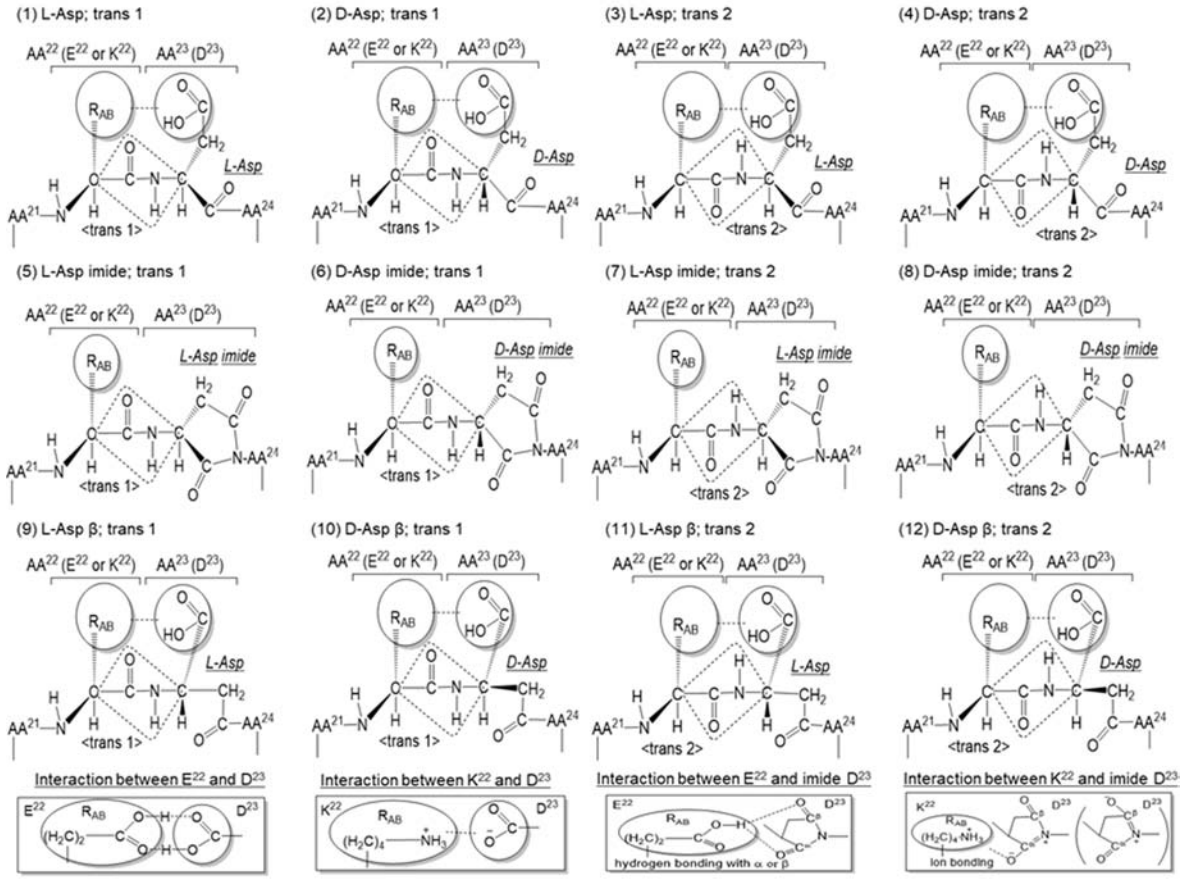

Figure 6. Chemical structures of the segmental peptides of Amyloid β42 wild-type and Italian mutant epimers having L-Asp or D-Asp at D^{23}. a) The structures trans 1 and trans 2 have different conformational peptide bonds. b) No. (1) to (4) are usual α-carboxy of Asp making a peptide bond. c) No. (5) to (8) are structures in which D^{23} residue has an imide structure. d) No. (9) to (12) are β-carboxy of Asp making a peptide bond. The interactions between the side chains of K^{22} and D^{23} are ion bonding or hydrogen bonding.

and AA^{23} are assumed to be hydrogen bonding between the side-chain carboxy group of E^{22} and D^{23}, and ionic bonding between the ammonium cation of K^{22} and carboxylate anion of D^{23}.

4.2. Comparing Clog *P* values of the segmental dipeptides of the wild-type Amyloid β42 with those of the Italian mutant

Values of Clog *P* for *N*-acetyl-Glutamic-Aspartic-amide, *N*-acetyl-Lysine-Aspartic-amide, and their derivatives including epimers are shown in Table 4 and Figure 7.

The compounds numbered D231 to D234 and KD231 to KD234 do not have the structure according to the interaction between the side chains but have protonated side chains. The amino acids possessing free carboxylate anion (Glu^- and Asp^-) have a little outlier from the relationship between Exptl. Log *P* and C log *P* as shown in Table 1 and Figure 3, whereas Exptl. Log *P* values of the protonated amino acids (GluH and AspH) may have better homology with Clog *P* values. Therefore, Clog *P* values of amino acids and peptides having protonated side chains must be more homologous to Exptl. Log *P* values. In this paper, the protonated side chains are considered as the typical model structure for the segmental peptides to estimate Exptl. Log *P* values. In Figure 7, the results of Clog *P* values are arranged comparing the results of the L-form epimers with that of the D-form epimer at D^{23}.

Observing the data for the structures based on the wild type of Amyloid β42, a little higher hydrophilicity can be seen in the models (D235 to D2312) formed by the interaction between the side chains than in the models (D231 to D234) formed without the interaction between the side chains. On the other hand, the Italian mutant segment models have inverse results compared with those of the wild-type segment. Values of Clog *P* of the models KD235 to KD2312 showed higher hydrophobicity than the models KD231 to KD234.

4.3. Comparing Clog *P* values of the segmental dipeptide imides of the wild-type Amyloid β42 with those of the Italian mutant

Table 5 and Figure 8 show the data about the dipeptide imide structures of the wild type and Italian mutant. The dipeptide imides of the wild type showed values in the range –2.80 to –2.10. The dipeptide imides of the Italian mutant showed values in the range –3.32 to –2.75. The dipeptide imides of the Italian mutant were generally more hydrophilic than those of the wild type. The larger and hydrophobic Clog *P* values for the dipeptide segments of the wild type were obtained in the imide models (D2313 to D2322) than in the straight models (D233 to D2312). The smaller and more hydrophilic Clog *P* values for the dipeptide segments of the Italian mutant were obtained in the imide models (KD2313 to KD2322) than in the straight models (KD235 to KD2312). D-epimers and L-epimers of the wild type gave similar Clog *P* values except for D2319 to D2322, which have hydrogen bonding between the β-carbonyl group of the imide and the side-chain carboxy group of GluH. Most of the L-epimers of the Italian mutant gave larger Clog *P* values than the D-epimers except for KD2319 and KD2320.

4.4. Comparing Clog *P* values of the segmental tripeptides of the wild-type Amyloid β42 with those of the Italian mutant

Table 6 and Figure 9 show data about the straight tripeptide structures of the wild type and Italian mutant of Amyloid β42. Comparing Clog *P* values of the wild type (D2323 to D2330) with those of the Italian mutant (KD2323 to KD2330), higher hydrophobicity can be seen in the Italian mutant (KD2323 to KD2330) (–1.53 to –0.44) than the models (D2323 to D2330) (–2.05 to –1.43) in the wild type. In the segments of the wild type, the D-epimer gave larger Clog *P* values than the L-epimer except for the pair of D2325 and D2326. In the segments of the Italian mutant, the D-epimer gave larger Clog *P* values than the L-epimer except for the pair of KD2325 and KD2326. These segmental peptides have the trans 2 structure.

4.5. Comparing Clog *P* values of the segmental tripeptide imides of the wild-type Amyloid β42 with those of the Italian mutant

Table 7 and Figure 10 show data for the tripeptide imide of the wild type and Italian mutant of Amyloid β42. Comparing Clog *P* values of the wild type (D2331 to D2338) with those of the

Table 4. Calculated log *P* values of dipeptides isomerized at D^{23} in the wild and Italian mutant of Amyloid β42.

No.	*N*-Acetyl-Peptide amides	A: Hf in vacuum (kcal/ mol)	B: Solvent accessible area ($Å^2$)	C: Hf in H_2O (kcal/ mol)	D: Number of N atom	E: Number of O atom	Clog P
D231	Ac-GluH-L-AspH-NH_2	-344.1	301.4	-378.5	3	7	-2.86
D232	Ac-GluH-D-AspH-NH_2	-341.0	312.7	-380.2	3	7	-2.76
D233	Ac-GluH-L-βAspH-NH_2	-340.5	321.6	-377.9	3	7	-2.52
D234	Ac-GluH-D-βAspH-NH_2	-339.9	322.2	-381.5	3	7	-2.62
D235	Ac-GluH-L-AspH-NH_2 trans1	-344.2	297.9	-374.5	3	7	-2.83
D236	Ac-GluH-D-AspH-NH_2 trans1	-344.2	296.6	-375.4	3	7	-2.88
D237	Ac-GluH-L-AspH-NH_2 trans2	-340.1	291.5	-375.1	3	7	-3.10
D238	Ac-GluH-D-AspH-NH_2 trans2	-340.3	288.7	-367.7	3	7	-2.96
D239	Ac-GluH-L-βAspH-NH_2 trans1	-342.4	283.3	-379.5	3	7	-3.33
D2310	Ac-GluH-D-βAspH-NH_2 trans1	-342.4	292.8	-379.8	3	7	-3.13
D2311	Ac-GluH-L-βAspH-NH_2 trans2	-342.3	291.8	-368.9	3	7	-2.87
D2312	Ac-GluH-D-βAspH-NH_2 trans2	-341.5	290.7	-371.0	3	7	-2.97
KD231	Ac-LysH-L-AspH-NH_2	-127.1	320.8	-197.6	4	5	-3.14
KD232	Ac-LysH-D-AspH-NH_2	-125.4	318.9	-194.9	4	5	-3.16
KD233	Ac-LysH-L-βAspH-NH_2	-119.9	325.9	-204.1	4	5	-3.42
KD234	Ac-LysH-D-βAspH-NH_2	-112.1	343.1	-205.6	4	5	-3.33
KD235	Ac-LysH-L-Asp-NH_2 trans1	-254.9	319.3	-318.6	4	5	-2.49
KD236	Ac-LysH-D-Asp-NH_2 trans1	-262.1	319.7	-308.0	4	5	-1.98
KD237	Ac-LysH-L-Asp-NH_2 trans2	-260.3	316.5	-309.6	4	5	-2.15
KD238	Ac-LysH-D-Asp-NH_2 trans2	-257.0	314.7	-298.3	4	5	-1.99
KD239	Ac-LysH-L-βAsp-NH_2 trans1	-260.4	317.6	-312.5	4	5	-2.20
KD2310	Ac-LysH-D-βAsp-NH_2 trans1	-259.9	314.1	-311.1	4	5	-2.25
KD2311	Ac-LysH-L-βAsp-NH_2 trans2	-257.1	314.9	-304.8	4	5	-2.15
KD2312	Ac-LysH-D-βAsp-NH_2 trans2	-255.7	320.1	-313.7	4	5	-2.32

Hf: Heat of formation; Clog P: Calculated log P.
GluH (Glutamic acid) and AspH (Aspartic acid) of which side chains protonated and liked with hydrogen bonding.
LysH (Lysine) and AspH (Aspartic acid) of which side chains are protonated and linked with ionic bonding.
All the amino acids without heading D- have L-chirality.; Aspimide has an imide structure.
Heading only β is β-carboxy of L-Asp making peptide bond with Ala residue.
Heading D-β is β-carboxy of D-Asp making peptide bond with Ala residue.

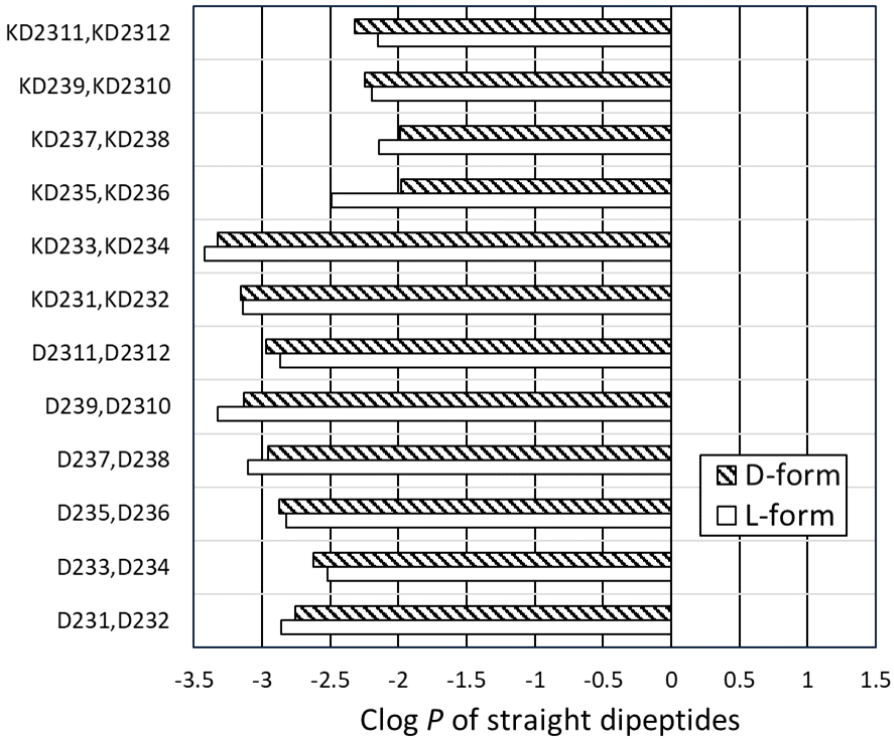

Figure 7. Comparison between Clog *P* values of the dipeptide segment models of Ac-E^{22}-D^{23}-NH_2 (the wild type of Amyloid β42) and Ac-K^{22}-D^{23}-NH_2 (Italian mutant) as well as between the L-epimer and D-epimer.

Table 5. Calculated log *P* values of dipeptide imides at D^{23} in the wild and Italian mutant of Amyloid β42.

No.	*N*-Acetyl-Peptide amides	A: Hf in vacuum (kcal/ mol)	B: Solvent accessible area ($Å^2$)	C: Hf in H_2O (kcal/ mol)	D: Number of N atom	E: Number of O atom	Clog P
D2313	Ac-GluH-L-Aspimide-NH	-282.6	305.3	-314.5	3	6	-2.26
D2314	Ac-GluH-D-Aspimide-NH	-281.9	305.2	-314.0	3	6	-2.26
D2315	Ac-GluH-L-AspimideαH-NH trans1	-278.8	302.8	-313.7	3	6	-2.40
D2316	Ac-GluH-D-AspimideαH-NH trans1	-280.5	293.9	-313.2	3	6	-2.53
D2317	Ac-GluH-L-AspimideαH-NH trans2	-277.5	295.6	-315.1	3	6	-2.64
D2318	Ac-GluH-D-AspimideαH-NH trans2	-275.4	301.5	-315.6	3	6	-2.59
D2319	Ac-GluH-L-AspimideβH-NH trans1	-282.6	303.3	-307.0	3	6	-2.10
D2320	Ac-GluH-D-AspimideβH-NH trans1	-281.6	301.2	-312.8	3	6	-2.36

Table 5 continued..

No.	*N*-Acetyl-Peptide amides	A: Hf in vacuum (kcal/ mol)	B: Solvent accessible area ($Å^2$)	C: Hf in H_2O (kcal/ mol)	D: Number of N atom	E: Number of O atom	Clog P
D2321	Ac-GluH-L-AspimideβH-NH trans2	-273.1	286.2	-308.9	3	6	-2.80
D2322	Ac-GluH-D-AspimideβH-NH trans2	-283.4	297.7	-316.7	3	6	-2.45
KD2313	Ac-LysH-L-Aspimide-NH	-44.4	325.1	-144.5	4	4	-3.32
KD2314	Ac-LysH-D-Aspimide-NH	-54.6	321.0	-144.3	4	4	-3.09
KD2315	Ac-LysH-L-AspimideαH-NH trans1	-65.6	304.7	-136.3	4	4	-2.89
KD2316	Ac-LysH-D-AspimideαH-NH trans1	-63.3	301.9	-126.1	4	4	-2.75
KD2317	Ac-LysH-L-AspimideαH-NH trans2	-63.8	301.3	-138.0	4	4	-3.07
KD2318	Ac-LysH-D-AspimideαH-NH trans2	-59.2	311.4	-136.1	4	4	-2.94
KD2319	Ac-LysH-L-AspimideβH-NH trans1	-63.6	318.3	-148.4	4	4	-2.98
KD2320	Ac-LysH-D-AspimideβH-NH trans1	-60.1	300.9	-132.7	4	4	-3.05
KD2321	Ac-LysH-L-AspimideβH-NH trans2	-46.1	303.9	-125.6	4	4	-3.22
KD2322	Ac-LysH-D-AspimideβH-NH trans2	-56.2	301.5	-130.8	4	4	-3.10

Hf: Heat of formation; Clog P: Calculated log P.
GluH (Glutamic acid) and AspH (Aspartic acid) of which side chains protonated and liked with hydrogen bonding except of D2313 and D2314. LysH (Lysine) and AspH (Aspartic acid) of which side chains are protonated and linked with ionic bonding except of KW2313 and KD2314. All the amino acids without heading D- have L-chirality. AspimideαH has an imide structure of which α-carbonyl oxygen makes a bonding with the side chain of GluH or LysH. AspimideβH has an imide structure of which β-carbonyl oxygen makes a bonding with the side chain of GluH or LysH. Heading only β is β-carboxy of L-Asp making peptide bond with Ala residue. Heading D-β is β-carboxy of D-Asp making peptide bond with Ala residue.

Italian mutant (KD2331 to KD2338), larger Clog *P* values can be seen in the models D2331 to D2338 (–2.14 to –1.14) in the wild type than in the Italian mutant (KD2331 to KD2338) (–2.20 to –1.80).

Comparing the Clog *P* values of the straight tripeptide and imide of the wild type, the Clog *P* values from the imide (D2331 to D2338) (–2.14 to –1.14) was a little larger than that of the straight tripeptides (D2323 to D2330) (–2.05 to –1.43) as shown in Table 6 and Figure 9. In the case of the Italian mutant, the Clog *P* values from the straight tripeptides (KD2323 to KD2330) (–1.53 to –0.44) was larger than that of the imide (KD2331 to KD2338) (–2.20 to –1.80) as shown in Table 6 and Figure 9. D-epimers and L-epimers gave different Clog *P* values depending on the structure.

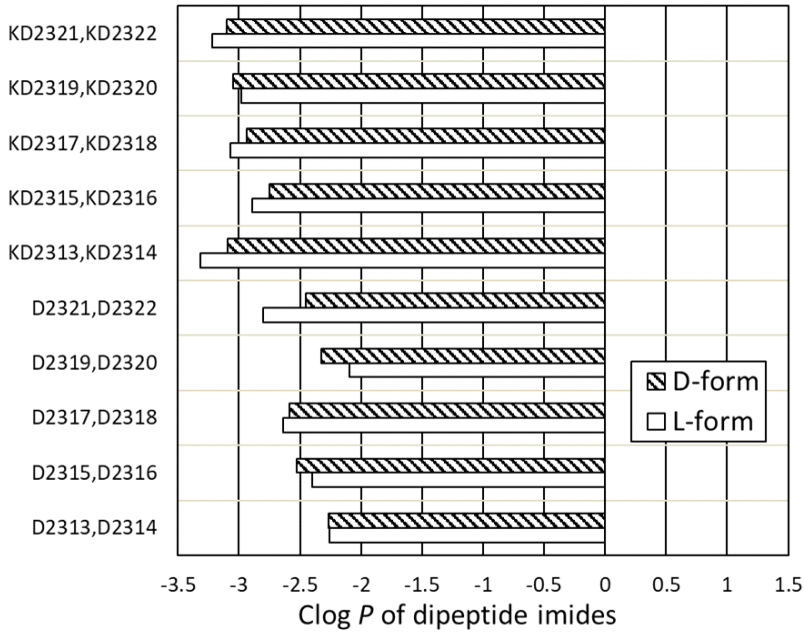

Figure 8. Clog *P* values of the dipeptide imide models of Ac-E^{22}-D^{23}-NH_2 (the wild type) and Ac-K^{22}-D^{23}-NH_2 (Italian mutant) as well as comparing the L-epimer and D-epimer.

Table 6. Calculated log *P* values of tripeptides isomerized at D^{23} in the wild and Italian mutant of Amyloid β42.

No.	*N*-Acetyl-Peptide amides	A: Hf in vacuum (kcal/ mol)	B: Solvent accessible area ($Å^2$)	C: Hf in H_2O (kcal/ mol)	D: Number of N atom	E: Number of O atom	Clog P
D2323	Ac-GluH-L-AspH-Val-NH_2 trans1	-393.9	387.4	-437.6	4	8	-2.05
D2324	Ac-GluH-D-AspH-Val-NH_2 trans1	-398.4	400.6	-433.7	4	8	-1.53
D2325	Ac-GluH-L-AspH-Val-NH_2 trans2	-395.5	407.2	-432.0	4	8	-1.43
D2326	Ac-GluH-D-AspH-Val-NH_2 trans2	-399.1	373.5	-431.5	4	8	-2.03
D2327	Ac-GluH-L-βAspH-Val-NH_2 trans1	-393.9	393.6	-438.3	4	8	-1.94
D2328	Ac-GluH-D-βAspH-Val-NH_2 trans1	-391.1	393.3	-432.2	4	8	-1.87
D2329	Ac-GluH-L-βAspH-Val-NH_2 trans2	-396.0	383.4	-428.9	4	8	-1.84
D2330	Ac-GluH-D-βAspH-Val-NH_2 trans2	-391.5	405.5	-433.5	4	8	-1.63
KD2323	Ac-LysH-L-Asp-Val-NH_2 trans1	-318.8	380.8	-361.0	5	6	-1.40

Table 6 continued..

No.	*N*-Acetyl-Peptide amides	A: Hf in vacuum (kcal/ mol)	B: Solvent accessible area ($Å^2$)	C: Hf in H_2O (kcal/ mol)	D: Number of N atom	E: Number of O atom	Clog P
KD2324	Ac-LysH-D-Asp-Val-NH_2 trans1	-320.5	409.5	-370.3	5	6	-0.98
KD2325	Ac-LysH-L-Asp-Val-NH_2 trans2	-319.3	394.4	-370.8	5	6	-1.35
KD2326	Ac-LysH-D-Asp-Val-NH_2 trans2	-312.9	394.2	-369.8	5	6	-1.53
KD2327	Ac-LysH-L-βAsp-Val-NH_2 trans1	-366.9	482.2	-432.6	6	7	-0.62
KD2328	Ac-LysH-D-βAsp-Val-NH_2 trans1	-367.4	464.8	-414.3	6	7	-0.48
KD2329	Ac-LysH-L-βAsp-Val-NH_2 trans2	-361.2	469.7	-409.0	6	7	-0.44
KD2330	Ac-LysH-D-βAsp-Val-NH_2 trans2	-360.8	479.4	-418.7	6	7	-0.50

Hf: Heat of formation; Clog P: Calculated log P.
GluH (Glutamic acid) and AspH (Aspartic acid) of which side chains protonated and liked with hydrogen bonding.
LysH (Lysine) and AspH (Aspartic acid) of which side chains are protonated and linked with ionic bonding.
Heading only β is β-carboxy of L-Asp making peptide bond with Ala residue.
Heading D-β is β-carboxy of D-Asp making peptide bond with Ala residue.

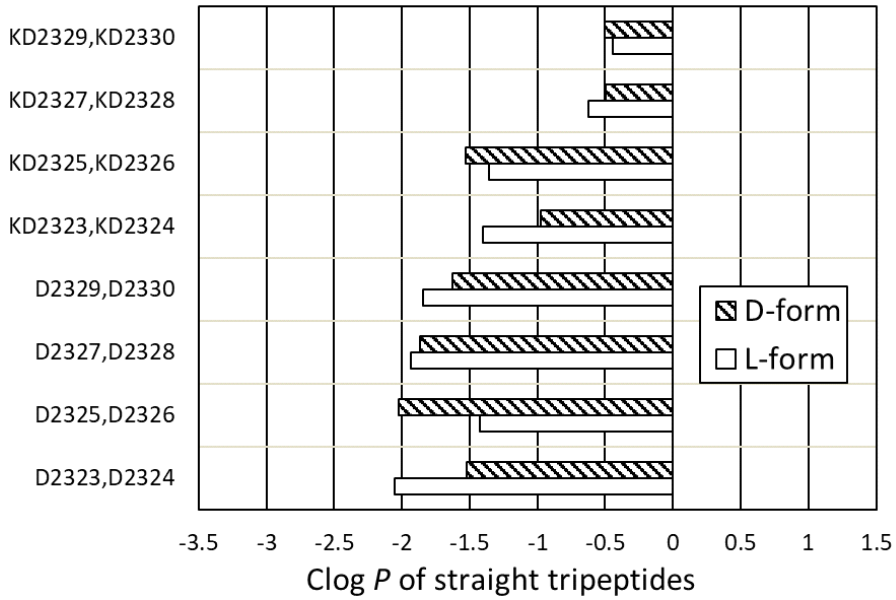

Figure 9. Clog *P* values of the tripeptide segment models of Ac-E^{22}-D^{23}-V^{24}-NH_2 (the wild type) and Ac-K^{22}-D^{23}-V^{24}-NH_2 (Italian mutant) as well as comparing the L-epimer and D-epimer.

Table 7. Calculated log *P* values of tripeptide imides at D^{23} in the wild and Italian mutant of Amyloid β42.

No.	*N*-Acetyl-Peptide amides	A: Hf in vacuum (kcal/ mol)	B: Solvent accessible area ($Å^2$)	C: Hf in H_2O (kcal/mol)	D: Number of N atom	E: Number of O atom	Clog P
D2331	Ac-GluH-L-AspimideαH-Val-NH_2 trans1	-335.2	389.4	-370.2	4	7	-1.36
D2332	Ac-GluH-D-AspimideαH-Val-NH_2 trans1	356.3	-377.5	-277.6	4	7	-2.14
D2333	Ac-GluH-L-AspimideαH-Val-NH_2 trans2	-333.3	384.5	-370.0	4	7	-1.52
D2334	Ac-GluH-D-AspimideαH-Val-NH_2 trans2	-336.9	362.5	-371.0	4	7	-1.91
D2335	Ac-GluH-L-AspimideβH-Val-NH_2 trans1	-337.9	362.4	-369.5	4	7	-1.84
D2336	Ac-GluH-D-AspimideβH-Val-NH_2 trans1	-338.9	393.7	-369.9	4	7	-1.14
D2337	Ac-GluH-L-AspimideβH-Val-NH_2 trans2	-331.8	372.7	-364.2	4	7	-1.66
D2338	Ac-GluH-D-AspimideβH-Val-NH_2 trans2	-331.4	364.7	-370.3	4	7	-2.01
KD2331	Ac-LysH-L-AspimideαH-Val-NH_2 trans1	-128.2	393.8	-196.5	5	5	-1.80
KD2332	Ac-LysH-D-AspimideαH-Val-NH_2 trans1	-135.5	375.1	-200.8	5	5	-2.10
KD2333	Ac-LysH-L-AspimideαH-Val-NH_2 trans2	-129.9	379.0	-200.4	5	5	-2.17
KD2334	Ac-LysH-D-AspimideαH-Val-NH_2 trans2	-130.0	390.7	-204.0	5	5	-2.02
KD2335	Ac-LysH-L-AspimideβH-Val-NH_2 trans1	-127.3	388.8	-207.5	5	5	-2.20
KD2336	Ac-LysH-D-AspimideβH-Val-NH_2 trans1	-117.1	396.1	-199.5	5	5	-2.17
KD2337	Ac-LysH-L-AspimideβH-Val-NH_2 trans2	-121.8	371.6	-177.2	5	5	-1.96
KD2338	Ac-LysH-D-AspimideβH-Val-NH_2 trans2	-113.7	375.0	-176.2	5	5	-2.11

Hf: Heat of formation; Clog P: Calculated log P.
GluH (Glutamic acid) and AspH (Aspartic acid) of which side chains protonated and liked with hydrogen bonding. LysH (Lysine) and AspH (Aspartic acid) of which side chains are protonated and linked with ionic bonding. All the amino acids without heading D- have L-chirality. AspimideαH has an imide structure of which α-carbonyl oxygen makes a bonding with the side chain of GluH or LysH. AspimideβH has an imide structure of which β-carbonyl oxygen makes a bonding with the side chain of GluH or LysH.
Heading only β is β-carboxy of L-Asp making peptide bond with Ala residue.
Heading Dβ is β-carboxy of D-Asp making peptide bond with Ala residue.

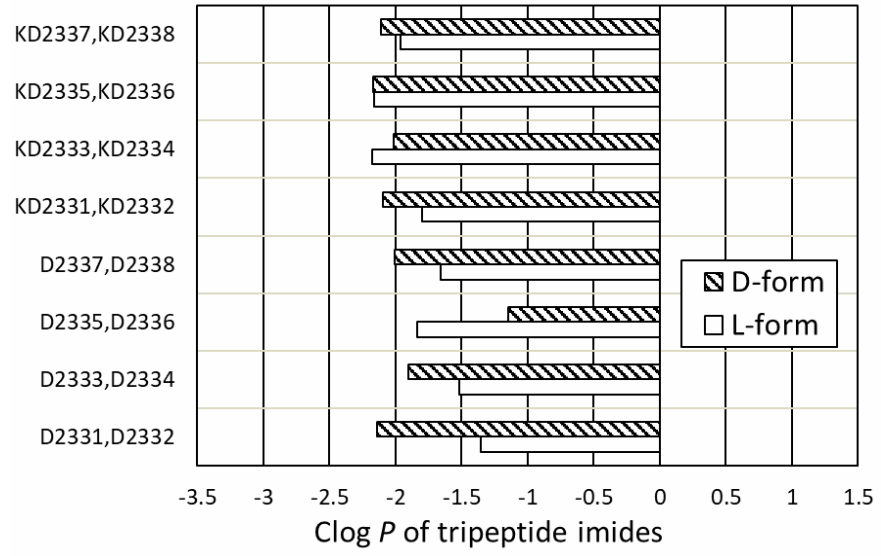

Figure 10. Clog *P* values of the tripeptide imide models of Ac-E^{22}-D^{23}-V^{24}-NH_2 (the wild type) and Ac-K^{22}-D^{23}-V^{24}-NH_2 (Italian mutant) as well as comparing the L-epimer and D-epimer.

4.6. Comparing Clog *P* values of the segmental tetrapeptides of the wild-type Amyloid β42 with those of the Italian mutant

Table 8 and Figure 11 show data for the straight tetrapeptide structures of the wild type and Italian mutant of Amyloid β42. Calculation was carried out for the segmental models having a hydrogen bond between C=O of Ala residue and NH of Val residue. Comparing Clog *P* values of the wild type (D2339 to D2346) with those of the Italian mutant (KD2339 to KD2346), higher hydrophobicity can be seen in the Italian mutant (KD2339 to KD2346) (–1.48 to –0.40) than in the models D2339 to D2346 (–2.18 to –1.35) in the wild type.

4.7. Comparing Clog *P* values of the segmental tetrapeptide imides of the wild-type Amyloid β42 with those of the Italian mutant

Table 9 and Figure 12 show data for the tetrapeptide imide of the wild type and Italian mutant of Amyloid β42. These segmental models have no hydrogen bond between C=O of Ala residue and NH of Val residue. Comparing Clog *P* values of the wild type (D2347 to D2354) with those of the Italian mutant (KD2347 to KD2354), a little larger hydrophobicity can be seen in the models D2347 to D2354 (–1.36 to –0.60) in the wild type than in the Italian mutant KD2347 to KD2354 (–2.10 to –1.18).

Comparing the Clog *P* values of the straight tetrapeptide and imide of the wild type, a little larger hydrophobicity as Clog *P* value was obtained from the imide (D2347 to D2354) (–1.36 to –0.60) than the straight tripeptides (D2339 to D2346) (–2.18 to –1.35). In the case of the Italian mutant, the larger hydrophobicity as Clog *P* value was obtained from the straight tripeptides KD2339 to KD2346 (–1.48 to –0.40) than from the imide KD2347 to KD2354 (–2.10 to –1.18). D-Epimers and L-epimers gave similar Clog *P* values.

4.8. Comparing Clog *P* values of the segmental hexapeptides of the wild type with those of the Italian mutant based on one or two hydrogen-bonding form

The segmental hexapeptides with one or two hydrogen bonds are shown in Figure 13. The chemical structures of the segmental hexapeptides are classified into several forms: (1) wild type or Italian mutant, (2) L-form or D-form with D^{23} chirality, (3) trans 1 or trans 2, (4) α-peptide or β-peptide, and (5) having one hydrogen bond (hydrogen bonding 1) or two hydrogen bonds (hydrogen bonding 1 and 2). These structures are constructed based on the assumption of the interaction between the side chain of AA^{22} and that of D^{23}.

Table 8. Calculated log *P* values of tetrapeptides isomerized at D^{23} in the wild and Italian mutant of Amyloid β42.

No.	*N*-Acetyl-Peptide amides	A: Hf in vacuum (kcal/ mol)	B: Solvent accessible area ($Å^2$)	C: Hf in H_2O (kcal/ mol)	D: Number of N atom	E: Number of O atom	Clog P
D2339	HB Ac-Ala-GluH-L-AspH-Val-NH_2 trans1	-457.4	421.1	-496.5	5	9	-1.86
D2340	HB Ac-Ala-GluH-D-AspH-Val-NH_2 trans1	-457.1	414.0	-495.8	5	9	-2.01
D2341	HB Ac-Ala-GluH-L-AspH-Val-NH_2 trans2	-454.5	447.1	-495.1	5	9	-1.35
D2342	HB Ac-Ala-GluH-D-AspH-Val-NH_2 trans2	-443.8	422.6	-494.0	5	9	-2.18
D2343	HB Ac-Ala-GluH-L-βAspH-Val-NH_2 trans1	-453.0	414.1	-494.7	5	9	-2.10
D2344	HB Ac-Ala-GluH-D-βAspH-Val-NH_2 trans1	-453.9	429.9	-492.6	5	9	-1.68
D2345	HB Ac-Ala-GluH-L-βAspH-Val-NH_2 trans2	-449.2	420.2	-490.6	5	9	-1.97
D2346	HB Ac-Ala-GluH-D-βAspH-Val-NH_2 trans2	-452.0	418.4	-490.3	5	9	-1.92
KD2339	HB Ac-Ala-LysH-L-AspH-Val-NH_2 trans1	-373.5	453.3	-426.1	6	7	-0.87
KD2340	HB Ac-Ala-LysH-D-AspH-Val-NH_2 trans1	-368.5	466.5	-424.4	6	7	-0.70
KD2341	HB Ac-Ala-LysH-L-AspH-Val-NH_2 trans2	-369.9	425.5	-422.2	6	7	-1.48
KD2342	HB Ac-Ala-LysH-D-AspH-Val-NH_2 trans2	-365.5	445.6	-422.1	6	7	-1.18
KD2343	HB Ac-Ala-LysH-L-βAspH-Val-NH_2 trans1	-371.9	442.1	-424.3	6	7	-1.12
KD2344	HB Ac-Ala-LysH-D-βAspH-Val-NH_2 trans1	-371.9	456.7	-409.0	6	7	-0.40
KD2345	HB Ac-Ala-LysH-L-βAspH-Val-NH_2 trans2	-365.3	454.7	-411.2	6	7	-0.70
KD2346	HB Ac-Ala-LysH-D-βAspH-Val-NH_2 trans2	-367.1	452.4	-433.7	6	7	-1.28

Hf: Heat of formation; Clog P: Calculated log P.
HB: Calculation was carried out for the segmental models having a hydrogen bond between C=O of Ala residue and NH of Val residue. GluH (Glutamic acid) and AspH (Aspartic acid) of which side chains protonated and liked with hydrogen bonding. LysH (Lysine) and AspH (Aspartic acid) of which side chains are protonated and linked with ionic bonding. All the amino acids without heading D- have L-chirality.
Heading only β is β-carboxy of L-Asp making peptide bond with Ala residue.
Heading D-β is β-carboxy of D-Asp making peptide bond with Ala residue.

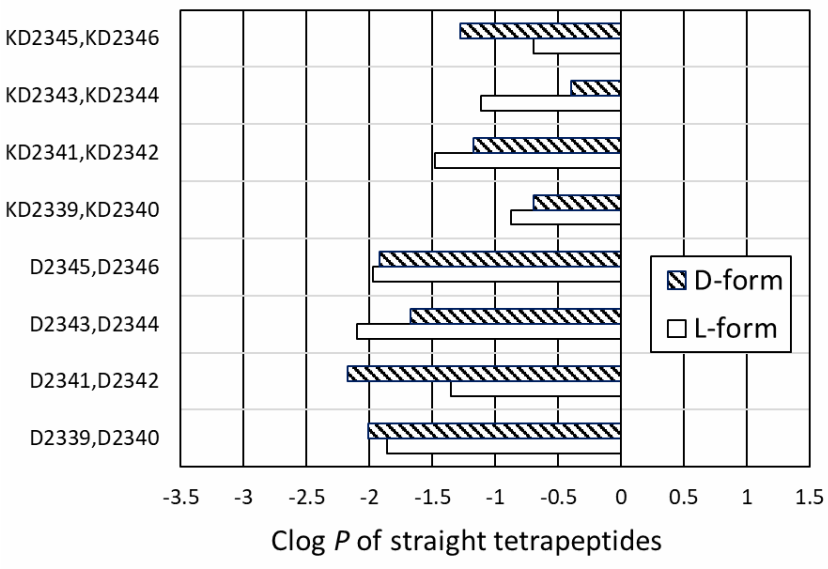

Figure 11. Clog *P* values of the tetrapeptide models of Ac-A^{21}-E^{22}-D^{23}-V^{24}-NH_2 (the wild type) and Ac-A^{21}-K^{22}-D^{23}-V^{24}-NH_2 (Italian mutant) as well as comparing the L-epimer and D-epimer.

Table 9. Calculated log *P* values of tetrapeptide imides at D^{23} in the wild and Italian mutant of Amyloid β42.

No.	*N*-Acetyl-Peptide amides	A: Hf in vacuum (kcal/ mol)	B: Solvent accessible area ($Å^2$)	C: Hf in H_2O (kcal/ mol)	D: Number of N atom	E: Number of O atom	Clog P
D2347	Ac-Ala-GluH-L-AspimideαH-Val-NH_2 trans1	-384.0	467.4	-425.2	5	8	-0.60
D2348	Ac-Ala-GluH-D-AspimideαH-Val-NH_2 trans1	-392.0	429.2	-432.2	5	8	-1.36
D2349	Ac-Ala-GluH-L-AspimideαH-Val-NH_2 trans2	-383.2	440.2	-425.4	5	8	-1.22
D2350	Ac-Ala-GluH-D-AspimideαH-Val-NH_2 trans2	-388.0	428.3	-422.0	5	8	-1.24
D2351	Ac-Ala-GluH-L-AspimideβH-Val-NH_2 trans1	-388.0	438.1	-424.4	5	8	-1.09
D2352	Ac-Ala-GluH-D-AspimideβH-Val-NH_2 trans1	-384.1	451.1	-427.4	5	8	-1.01
D2353	Ac-Ala-GluH-L-AspimideβH-Val-NH_2 trans2	-381.7	470.6	-432.6	5	8	-0.80
D2354	Ac-Ala-GluH-D-AspimideβH-Val-NH_2 trans2	-383.5	441.1	-428.2	5	8	-1.26
KD2347	Ac-Ala-LysH-L-AspimideαH-Val-NH_2 trans1	-177.1	473.5	-257.0	6	6	-1.24
KD2348	Ac-Ala-LysH-D-AspimideαH-Val-NH_2 trans1	-180.5	454.3	-247.6	6	6	-1.29

Table 9 continued..

No.	*N*-Acetyl-Peptide amides	A: Hf in vacuum (kcal/ mol)	B: Solvent accessible area ($Å^2$)	C: Hf in H_2O (kcal/ mol)	D: Number of N atom	E: Number of O atom	Clog P
KD2349	Ac-Ala-LysH-L-AspimideαH-Val-NH_2 trans2	-182.9	456.3	-253.1	6	6	-1.33
KD2350	Ac-Ala-LysH-D-AspimideαH-Val-NH_2 trans2	-171.5	462.6	-253.5	6	6	-1.55
KD2351	Ac-Ala-LysH-L-AspimideβH-Val-NH_2 trans1	-180.3	467.7	-254.0	6	6	-1.18
KD2352	Ac-Ala-LysH-D-AspimideβH-Val-NH_2 trans1	-170.6	453.6	-232.1	6	6	-1.20
KD2353	Ac-Ala-LysH-L-AspimideβH-Val-NH_2 trans2	-167.4	471.9	-249.1	6	6	-1.35
KD2354	Ac-Ala-LysH-D-AspimideβH-Val-NH_2 trans2	-157.9	445.6	-245.0	6	6	-2.10

Hf: Heat of formation; Clog P: Calculated log P.
GluH (Glutamic acid) and AspH (Aspartic acid) of which side chains protonated and liked with hydrogen bonding. LysH (Lysine) and AspH (Aspartic acid) of which side chains are protonated and linked with ionic bonding. All the amino acids without heading D- have L-chirality. AspimideαH has an imide structure of which α-carbonyl oxygen makes a bonding with the side chain of GluH or LysH.AspimideβH has an imide structure of which β-carbonyl oxygen makes a bonding with the side chain of GluH or LysH.
Heading only β is β-carboxy of L-Asp making peptide bond with Ala residue.
Heading D-β is β-carboxy of D-Asp making peptide bond with Ala residue.

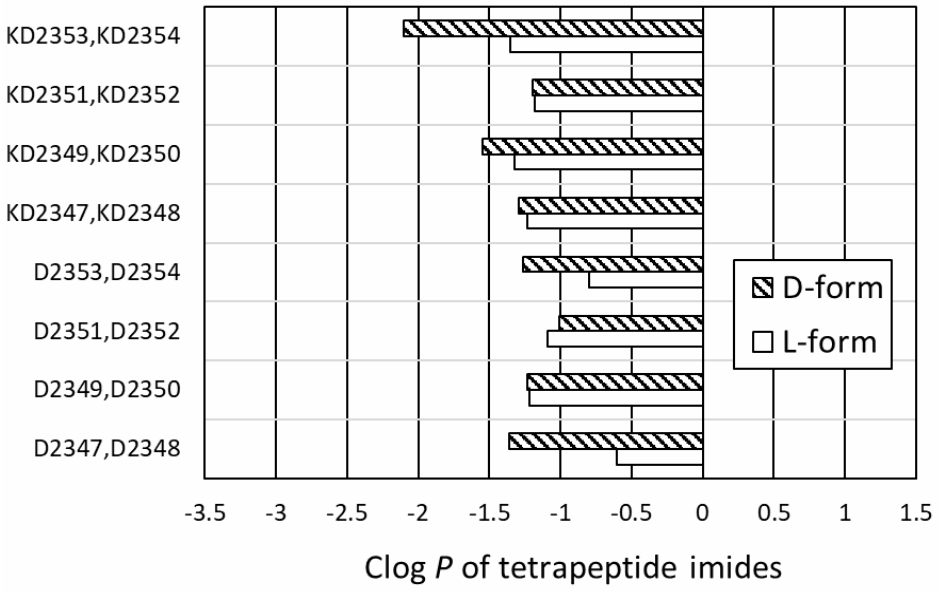

Figure 12. Clog *P* values of the tetrapeptide imide models of Ac-A^{21}-E^{22}-D^{23}-V^{24}-NH_2 (the wild type) and Ac-A^{21}-K^{22}-D^{23}-V^{24}-NH_2 (Italian mutant) as well as comparing the L-epimer and D-epimer.

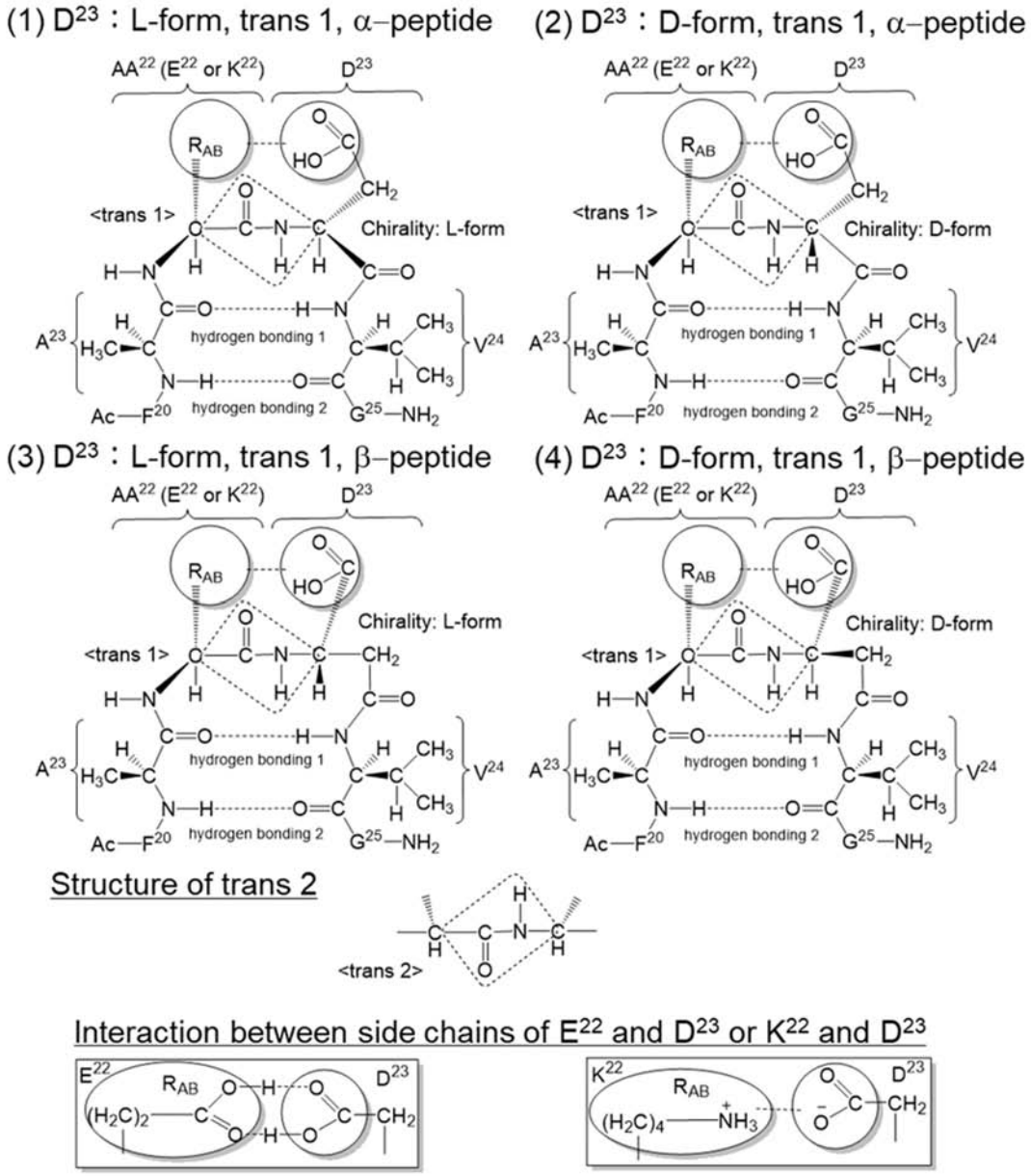

Figure 13. Chemical structures of the segmental hexapeptides of Amyloid β42 wild type and Italian mutant epimers having L-Asp or D-Asp at D^{23}.

In the case where AA^{22} is E^{22}, the interaction is hydrogen bonding between two carboxy groups. In the case where AA^{22} is K^{23}, the interaction is ionic bonding between ammonium and carboxylate ions.

Table 10 and Figure 14 show data for the straight hexapeptide of the wild type and Italian mutant of Amyloid β42. Comparing Clog *P* values of the wild type (D2355 to D2362) with those of the Italian mutant (KD2355 to KD2362), the higher hydrophobicity can be seen in the Italian mutant KD2355 to KD2362 (0.62 to 1.48) than in the models D2355 to D2362 (–0.89 to –0.13) in the wild type. Most of the D-epimers ((–0.52 to –0.13) and (0.71 to 1.48)) have higher Clog *P* values than those of the L-epimers ((–0.48 to –0.89) and (0.62 to 1.01)) of the wild type and Italian mutant, respectively.

Table 10. Calculated log *P* values of hexapeptides isomerized at D^{23} in the wild and Italian mutant of Amyloid β42 in case of possessing one hydrogen bond between A^{21} and V^{24}.

No.	*N*-Acetyl-Peptide amides	A: Hf in vacuum (kcal/mol)	B: Solvent accessible area (Å^2)	C: Hf in H_2O (kcal/ mol)	D: Number of N atom	E: Number of O atom	Clog P
D2355	HB Ac-FAEDVG-NH_2 trans1	-522.6	551.8	-564.0	7	11	-0.50
D2356	HB Ac-FAE(D)DVG-NH_2 trans1	-527.9	554.4	-561.9	7	11	-0.23
D2357	HB Ac-FAEDVG-NH_2 trans2	-523.5	557.1	-572.6	7	11	-0.59
D2358	HB Ac-FAE(D)DVG-NH_2 trans2	-523.9	572.4	-568.1	7	11	-0.13
D2359	HB Ac-FAED(β)VG-NH_2 trans1	-527.3	543.4	-561.7	7	11	-0.48
D2360	HB Ac-FAE(D)D(β)VG-NH_2 trans1	-525.2	560.5	-563.4	7	11	-0.22
D2361	HB Ac-FAED(β)VG-NH_2 trans2	-517.6	536.4	-560.6	7	11	-0.89
D2362	HB Ac-FAE(D)D(β)VG-NH_2 trans2	-519.6	553.0	-562.4	7	11	-0.52
KD2355	HB Ac-FAKDVG-NH_2 trans1	-432.6	611.7	-496.2	8	9	0.74
KD2356	HB Ac-FAK(D)DVG-NH_2 trans1	-430.5	623.0	-494.7	8	9	0.96
KD2357	HB Ac-FAKDVG-NH_2 trans2	-436.8	602.9	-498.2	8	9	0.62
KD2358	HB Ac-FAK(D)DVG-NH_2 trans2	-432.7	639.9	-491.2	8	9	1.48
KD2359	HB Ac-FAKD(β)VG-NH_2 trans1	-427.2	657.6	-516.9	8	9	1.01
KD2360	HB Ac-FAK(D)D(β)VG-NH_2 trans1	-417.7	607.7	-477.0	8	9	0.71
KD2361	HB Ac-FAKD(β)VG-NH_2 trans2	-442.2	596.1	-497.7	8	9	0.65
KD2362	HB Ac-FAK(D)D(β)VG-NH_2 trans2	-444.3	633.2	-510.9	8	9	1.17

Hf: Heat of formation; Clog P: Calculated log P.

HB: one hydrogen bond in the β-sheet structure.

E (Glutamic acid) and D (Aspartic acid) of which side chains protonated and liked with hydrogen bonding.

K (Lysine) and D (Aspartic acid) of which side chains are protonated and linked with ionic bonding.

All the amino acids without heading (D) have L-chirality. (D)D: D-Asp; D(β): L-βAsp; (D)D(β): D-βAsp.

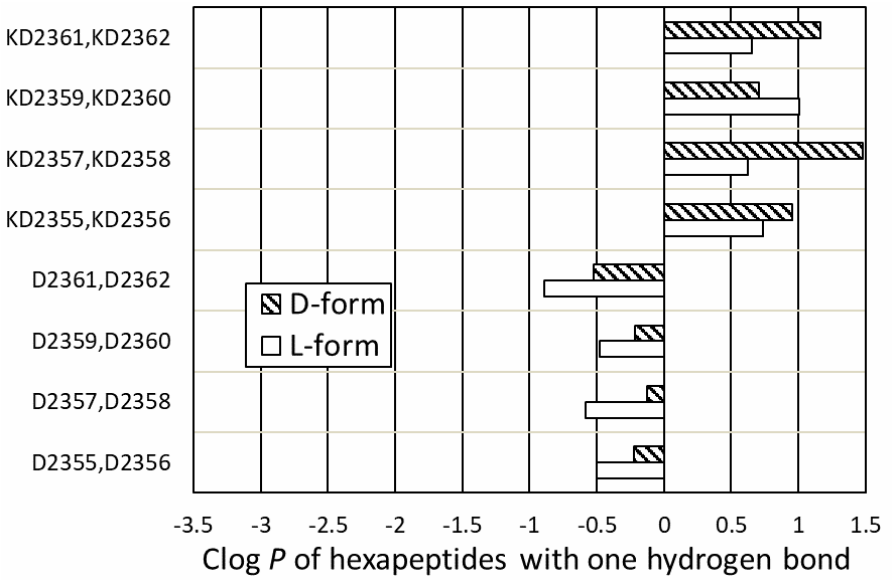

Figure 14. Clog *P* values of the hexapeptide models of Ac-F^{20}-A^{21}-E^{22}-D^{23}-V^{24}-G^{25}-NH_2 (the wild type) and Ac-F^{20}-A^{21}-K^{22}-D^{23}-V^{24}-G^{25}-NH_2 (Italian mutant) as well as comparing the L-epimer and D-epimer.

Table 11 and Figure 15 show data for the hexapeptide models of the wild type and Italian mutant of Amyloid β42. Comparing Clog *P* values of the wild type (D2363 to D2370) with those of the Italian mutant (KD2363 to KD2370), a little larger hydrophobicity can be seen in the models D2363 to D2370 (–0.70 to 0.05) in the wild type than in the Italian mutant KD2363 to KD2370 (0.32 to 1.32).

Most of the D-epimers ((–0.23 to 0.04) and (0.35 to 1.32)) have higher Clog *P* values than those of the L-epimers ((–0.70 to 0.05) and (0.32 to 0.92)) of the wild type and Italian mutant, respectively.

4.9. Comparing Clog *P* values of the segmental peptide models of the wild type with those of the Italian mutant from the viewpoint of the number of sequences

Figure 16 summarizes the calculation results of Clog *P* values of the segmental peptide models for the wild type. The data are shown as three columns that give minimum, average, and maximum calculation results for the segmental peptides. For example, D232-2311 (L5) means five models (having hydrogen bonding or not between side chains, trans 1 or trans 2, α-peptide or β-peptide) possessing L-chirality in the segmental peptides D232 to D2311, and D2314-2322 (D5) means five models possessing imide structures and D-chirality in the segmental peptides D2314 to D2322. These models are dipeptides. The columns positioned in the area separated by dashed lines show the data for models for dipeptides, tripeptides, tetrapeptides, and hexapeptides.

Clog *P* values of the models increased slightly with the larger peptides. Comparing the Clog *P* values of the models having the same amino acid numbers, the values for the straight peptide models were usually larger than those for the imide models. Compared with the results of L-epimer and D-epimer having the same peptide size, a similar Clog *P* value was observed in most sizes of peptides except for hexapeptides, which showed larger Clog *P* values in D-epimers than in L-epimers. These results suggest that the epimerization at D^{23} in the hexapeptides or longer segmental peptides would facilitate further hydrophobicity to reach aggregation.

Figure 17 summarizes the calculation results of Clog *P* values of the segmental peptide models of the Italian mutant. In the same way as Figure 16, the data are shown as three columns that contain minimum, average, and maximum of the calculation results for the segmental peptides.

Table 11. Calculated log *P* values of hexapeptides isomerized at D^{23} in the wild and Italian mutant of Amyloid β42 in case of possessing two hydrogen bonds between A^{21} and V^{24}.

No.	*N*-Acetyl-Peptide amides	A: Hf in vacuum (kcal/ mol)	B: Solvent accessible area (Å^2)	C: Hf in H_2O (kcal/ mol)	D: Number of N atom	E: Number of O atom	Clog P
D2363	2HB Ac-FAEDVG-NH_2 trans1	-521.9	551.6	-558.8	7	11	-0.41
D2364	2HB Ac-FAE(D)DVG-NH_2 trans1	-524.3	541.9	-565.2	7	11	-0.12
D2365	2HB Ac-FAEDVG-NH_2 trans2	-522.7	571.1	-559.0	7	11	0.05
D2366	2HB Ac-FAE(D)DVG-NH_2 trans2	-524.4	560.2	-562.8	7	11	-0.23
D2367	2HB Ac-FAED(β)VG-NH_2 trans1	-527.1	548.3	-557.6	7	11	-0.27
D2368	2HB Ac-FAE(D)D(β)VG-NH_2 trans1	-522.3	577.7	-564.5	7	11	0.04
D2369	2HB Ac-FAED(β)VG-NH_2 trans2	-517.5	550.4	-564.6	7	11	-0.70
D2370	2HB Ac-FAE(D)D(β)VG-NH_2 trans2	-522.9	565.6	-559.9	7	11	-0.09
KD2363	2HB Ac-FAKDVG-NH_2 trans1	-437.1	606.4	-502.6	8	9	0.32
KD2364	2HB Ac-FAK(D)DVG-NH_2 trans1	-441.0	622.0	-492.2	8	9	1.32
KD2365	2HB Ac-FAKDVG-NH_2 trans2	-438.6	594.6	-499.0	8	9	0.48
KD2366	2HB Ac-FAK(D)DVG-NH_2 trans2	-438.1	633.0	-508.4	8	9	1.04
KD2367	2HB Ac-FAKD(β)VG-NH_2 trans1	-426.9	641.9	-507.2	8	9	0.92
KD2368	2HB Ac-FAK(D)D(β)VG-NH_2 trans1	-426.5	595.7	-488.3	8	9	0.42
KD2369	2HB Ac-FAKD(β)VG-NH_2 trans2	-422.9	621.8	-507.8	8	9	0.35
KD2370	2HB Ac-FAK(D)D(β)VG-NH_2 trans2	-431.9	598.3	-485.5	8	9	0.71

Hf: Heat of formation; Clog P: Calculated log P.
2HB: two hydrogen bonds in the β-sheet structure.
E (Glutamic acid) and D (Aspartic acid) of which side chains protonated and liked with hydrogen bonding.
K (Lysine) and D (Aspartic acid) of which side chains are protonated and linked with ionic bonding.
All the amino acids without heading (D) have L-chirality. (D)D: D-Asp; D(β): L-βAsp; (D)D(β): D-βAsp.

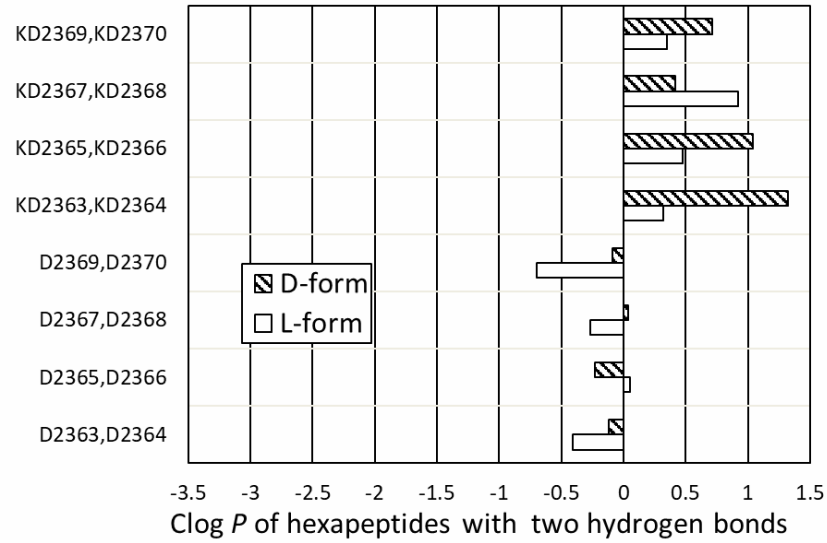

Figure 15. Clog *P* values of the two hydrogen-bonding models of hexapeptide of Ac-F^{20}-A^{21}-E^{22}-D^{23}-V^{24}-G^{25}-NH_2 (the wild type) and Ac-F^{20}-A^{21}-K^{22}-D^{23}-V^{24}-G^{25}-NH_2 (Italian mutant) as well as comparing the L-epimer and D-epimer.

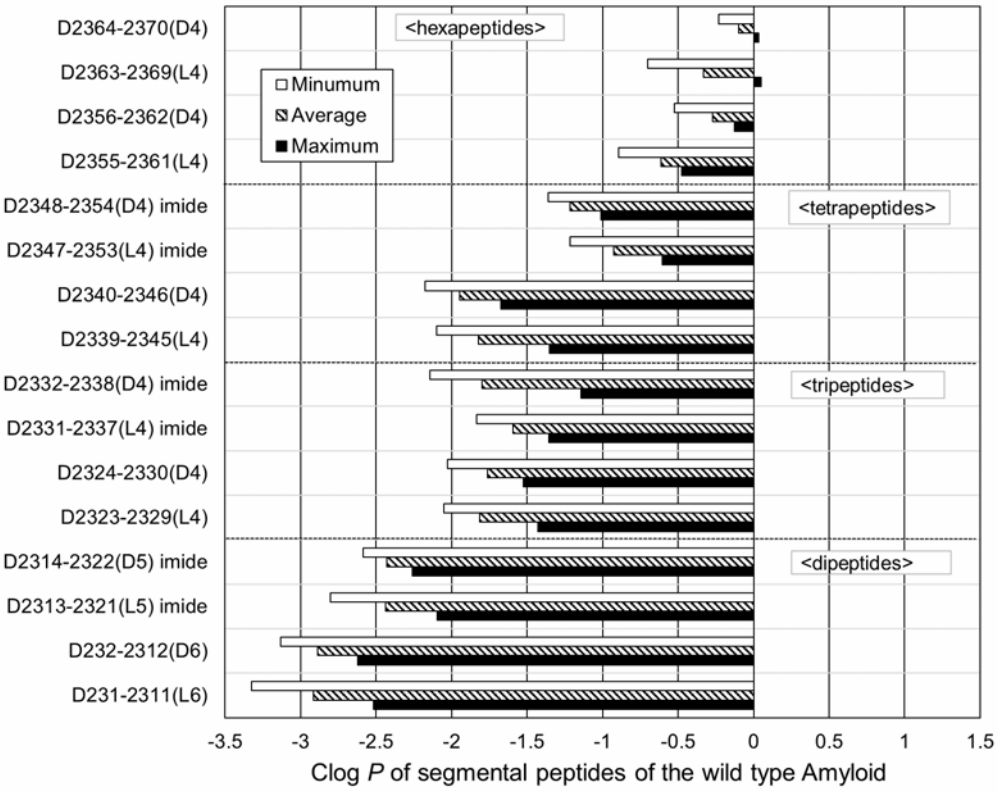

Figure 16. Clog *P* values of the segmental peptides of the wild type of Amyloid β42.
The three grouped columns present the data for minimum, average, and maximum Clog *P* values according to each categorized chemical structure. For instance, D2323-2329 (L4) are composed of four L-epimer tripeptide structures: D2323, D2325, D2327, and D2329.

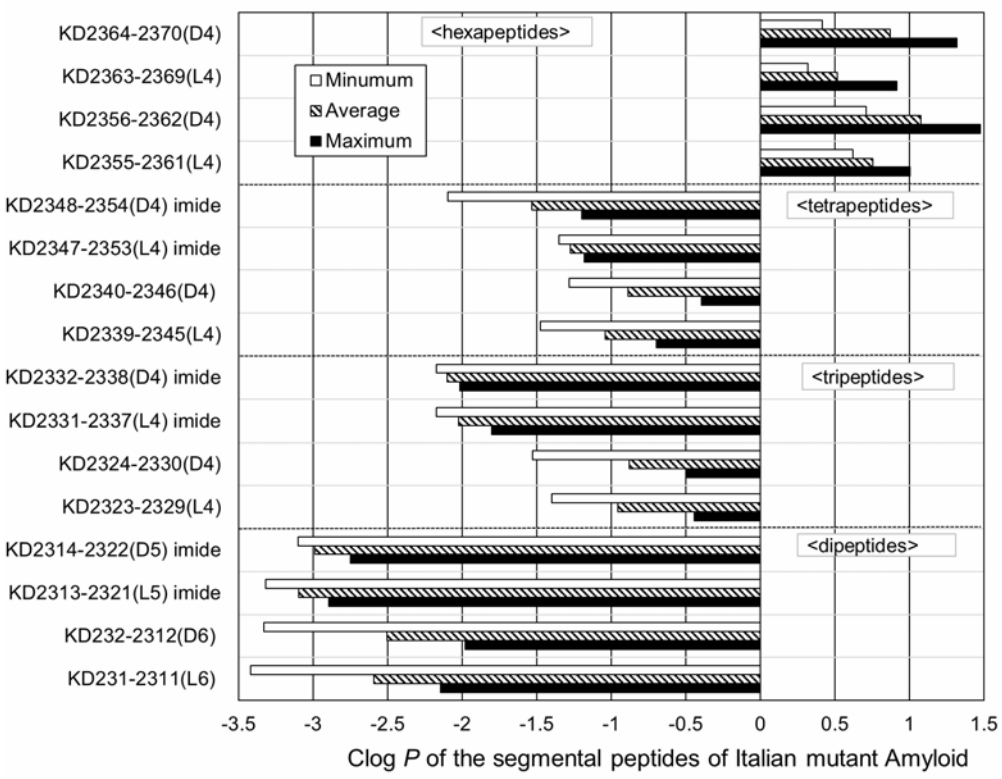

Figure 17. Clog *P* values of the segmental peptides of the Italian mutant of Amyloid β42.
The three grouped columns present the data for minimum, average, and maximum Clog *P* values according to each categorized chemical structure. For instance, KD232-2312 (D6) are composed of six D-epimer dipeptide structures: KD232, KD234, KD236, KD238, KD2310, and KD2312.

However, Figure 17 shows the data for the Italian mutant segmental models numbered KD231-2311 (L6) and KD232-2312 (D6). Naming of the segmental models and arranging the data in Figure 17 are presented similarly to those in Figure 16.

Comparing the straight structure of the peptides, Clog *P* values of the models increased slightly for the larger peptides. Although the Clog *P* value of imides also increased with the larger ones, Clog *P* values of the straight models were larger than those of imide models.

The results reveal that the imides of the wild type are more hydrophobic than their straight peptides, but the straight peptides of the Italian mutant are more hydrophobic than the imide models. Clog *P* values of the L-epimer and D-epimer are similar when compared to Clog *P* values of the same size of peptides: dipeptides, tripeptides, or tetrapeptides. However, in the data of tetrapeptide models, larger Clog *P* values were obtained in the D-epimer rather than in the L-epimer. All the results in hexapeptide models of the Italian mutant gave positive and much higher values than those in the hexapeptide models of the wild type as shown in Figure 16.

The calculation results demonstrate that if the epimerization occurred at the D^{23} position of the wild-type Amyloid β42 from L to D, the segmental hexapeptide area before and after D^{23} must be more hydrophobic. If the epimerization occurred at the D^{23} position of the Italian mutant from L to D, the same area before and after D^{23} must also be more hydrophobic. The resulting hydrophobicity ($0.5 < \text{Clog } P < 1$) of the epimerized segments of the Italian mutant must be much higher than those ($-0.7 < \text{Clog } P < 0$) of the wild type. Such results suggest that epimerization at D^{23} in the wild type and Italian mutant Amyloid β42 would make these more hydrophobic and would lead to more aggregation features.

CONCLUSIONS

A linear relationship (R^2 = 0.978) between Exptl. log *P* (logarithm of partition coefficient of octanol in water) and Clog *P* values for amino acids and *N*-acetyl-peptide amides was obtained by a semiempirical method using PM5 for estimating the hydrophobicity of the segmental peptide models of Amyloid β42.

It was suggested by the Clog *P* calculation that epimerization at D^1 and D^7 as the common residues with the wild type and Italian mutant of Amyloid β42 will make the original L-peptides more hydrophilic.

Clog *P* values for the segmental models (*N*-acetyl-peptide-NH_2) of dipeptides, tripeptides, tetrapeptides, and hexapeptides around the bending position at D^{23} were calculated. Clog *P* values became larger with the larger peptides except for the imide structures.

Clog *P* values for the straight segment peptides of the Italian mutant were larger than those of the wild type of Amyloid β42. The results may correspond to the higher aggregation of the whole structure of the Italian mutant than the wild type of Amyloid β42 because the higher hydrophobicity at the bending area may make the whole structure more hydrophobic.

Segmental hexapeptide models based on the K^{22}-D^{23} salt bridge and epimerization at the D^{23} residue gave larger Clog *P* values than those of L-hexapeptides. The results suggested that the Italian mutant will be more hydrophobic than the original one if epimerization occurred at D^{23}.

CONFLICT OF INTEREST STATEMENT

The author has no conflicts of interest directly relevant to the content of this article.

REFERENCES

1. Dyakin, V. V., Wisniewski, T. M. and Lajtha, A. 2021, Symmetry, 13, 455.
2. Yoshimura, T., Nishikawa, T. and Homma, H. 2016, “D-Amino Acids Physiology, Metabolism, and Application”, Springer Japan.
3. Konno, R., Brückner, H., D’Aniello, A., Fisher, G. and Fujii, N. 2009, “D-Amino Acids: Practical Methods and Protocols: D-amino Acids in Peptides and Proteins”, Nova Science Publishers Inc., Hauppauge, NY.
4. Konno, R., Brückner, H., D’Aniello, A., Fisher, G., Fujii, N. and Homma, H. 2007, “D-Amino Acids: A New Frontier in Amino Acid and Protein Research-Practical Methods and Protocols”, Nova Science Publishers Inc., Hauppauge, NY.
5. Montecucchi, P. C., Castiglione, R., Piani, S., Gonzzini, L. and Erspamer, V. 1981, Int. J. Pept. Prot. Res., 17, 275.
6. Broccardo, M., Erspamer, V., Erspamer, F. G., Improta, G., Linari, G., Melchiorri, P. and Montecucchi, P. C. 1981, Br. J. Pharmacol., 73, 625.
7. Fisher, H., Garcia, N. M., Payan, I. L., Cadilla-Perezrois, R., Sheremata, W. A. and Man, E. H. 1986, Biochem. Biophys. Res. Commun., 135, 683.
8. Richter, K., Egger, R. and Kreil, G. 1987, Science, 238, 200.
9. Erspamer, V., Melchiorri, P., Falconieri-Erspamer, G., Negri, L., Corsi, R., Severini, C., Barra, D., Simmaco, M. and Kreil, G. 1989, Proc. Natl. Acad. Sci. USA, 86, 5188.
10. Kamatani, Y., Minakata, H., Kenney, P. T., Iwashita, T., Watanabe, K., Funase, K., Sun, X. P., Yongsiri, A., Kim, K. H., Novales-Li, P., Novales, E. T., Kanapi, C. G., Takeuchi, H. and Nomoto, K. 1989, Biochem. Biophys. Res. Commun., 160, 1015.
11. Jolles, P. 1998, “D-Amino Acid in Sequences of Secreted Peptides of Multicellular Organisms”, Birkhauser Verlag, Basel.
12. Kumada, M., Teramoto, T., Kumagaye, K., Nakajima, K., Watanabe, T., Kawai, T., Kawakami, Y., Niidome, T., Sawada, K. and Nishizawa, Y. 1994, Mol. Pharmacol., 46, 587.
13. Heck, S. D., Siok, C. J., Krapcho, K. J., Kelbaugh, P. R., Thadeio, P. F., Welch, M. J., Williams, R. D., Ganong, A. H., Kelly, M. E., Lanzetti, A. J., William, R. G., Phillips, D., Parks, T. N., Jackson, H., Ahlijanian, M. K., Saccomano, N. A. and Volkmann, R. A. 1994, Science, 266, 1065.

14. Masuda, W., Nouso, C., Kitamura, C., Terashita, M. and Noguchi, T. 2002, Arch. Oral. Biol., 47, 757.
15. Cloos, P. A. and Fledelius, C. 2000, Biochem. J., 345, 473.
16. Powell, J. T., Vine, N. and Grossman, M. 1992, Atherosclerosis, 97, 201.
17. Rocher, A. E., Lowenson, J. D., Clarke, S., Walkow, C., Wang, R., Cotter, R. J., Reardon, I. M., Zurcher-Neely, H. A., Heinrikson, R. L., Ball, M. J. and Greenberg, B. D. 1993, J. Biol. Chem., 268, 3072.
18. Masters, P. M., Bada, J. L. and Zigler, J. S. J. 1977, Nature, 268, 71.
19. Momose, Y., Fujii, N., Kodama, T., Tamagaki, Y., Nakanishi, H. and Kodama, M. 1998, Viva Origino, 26, 329.
20. Fujii, N. and Saito, T. 2004, Chem. Record, 4, 267.
21. Fujii, N., Tajima, S., Tanaka, N., Fujimoto, N., Takaka, T. and Shimo-oka, T. 2002, Biochem. Biophys. Res. Commun., 294, 1047.
22. Ritz-Timme, S., Laumeier, I. and Collins, M. J. 2003, Br. J. Dermatol., 149, 951.
23. Shapiro, S. D., Endicott, S. K., Province, M. A., Pierce, J. A. and Campbell, E. J. 1991, J. Clin. Invest., 87, 1828.
24. Kaneko, I., Yamada, N., Sakuraba, Y., Kamenosono, M. and Tutumi, S. 1995, J. Neurochem., 65, 2585.
25. Munegumi, T. and Shimoyama, A. 2003, Chirality, 15, S108.
26. Munegumi, T. 2010, Chemistry & Biodiversity, 7, 1670.
27. Smith, G. G. and Reddy, G. V. 1989, J. Org. Chem., 54, 4529.
28. Liardon, R. and Hurrell, R. F. 1983, J. Agric. Food Chem., 31, 432.
29. Fujii, N., Muraoka, S., Satoh, K., Hori, H. and Harada, K. 1991, Biomed. Res., 12, 315.
30. Xie, M., Velde, D. V., Morton, M., Borchardt, R. T. and Schowen, R. L. 1996, J. Am. Chem. Soc., 118, 8955.
31. Radkiewicz, J. L., Zipse, H., Clarke, S. and Houk, K. N. 1996, J. Am. Chem. Soc., 118, 9148.
32. Catak, S., Monard, G., Aviyente, V. and Ruiz-Lopez, M. F. 2009, J. Phys. Chem. A, 113, 1111.
33. Bodor, H. and Huang, M. J. 1991, J. Comp. Chem., 12, 1182.
34. Kroeff, E. P. and Pietrzyk, D. J. 1978, Anal. Chem., 50, 502.
35. Kroeff, E. P. and Pietrzyk, D. J. 1978, Anal. Chem., 50, 1353.
36. Schwendinger, M. G. and Rode, B. M. 1992, Orig. Life, 22, 349.
37. Mitchell, A. R., Kent, S. B. H., Chu, I. C. and Merrifield, R. B. 1978, Anal. Chem., 50, 637.
38. Miyake, K. and Terada, H. 1978, J. Chromatogr., 157, 386.
39. Miyake, K., Mizuno, N. and Terada, H. 1986, Chem. Pharm. Bull., 34, 4787.
40. Albert, L., Hansch, C. and Elkins, D. 1971, Chem. Rev., 71, 525.
41. Carlson, R. M., Carlson, R. T. and Herbert, L. K. 1975, J. Chromatogr., 107, 219.
42. McCall, J. M. 1975, J. Med. Chem., 18, 549.
43. Mirrlees, M. S., Moulton, S. J., Murphy, C. T. and Taylor, P. J. 1976, J. Med. Chem., 19, 615.
44. Henry, D., Block, J. H., Anderson, J. L. and Carlson, G. R. 1976, J. Med. Chem., 19, 619.
45. Tanaka, N., Goodell, H. and Karger, B. L. 1978, J. Chromatogr., 158, 233.
46. Sangster, J. 1997, “Octanol–Water Partition Coefficients: Fundamentals and Physical Chemistry”, John Wiley & Sons, New York.
47. LOGKOW Sangster Research Laboratories, http://logkow.cisti.nrc.ca/logkow/index.jsp
48. Lundanes, E. and Greibrokk, T. 1978, J. Chromatogr., 149, 241.
49. Benfenati, E., Gini, G., Piclin, N., Roncaglioni, A. and Vari, M. R. 2003, Chemosphere, 53, 1155.
50. Stewart, J. J. C. 2007, J. Mol. Model., 13, 1173.
51. Murakami, K., Irie, K., Morimoto, A., Ohigashi, H., Shindo, M., Nagao, M., Shimizu, T. and Shirasawa, T. 2003, J. Biol. Chem., 278, 46179.
52. Roher, A. E., Lowenson, J. D., Clarke, S., Wolkow, C., Wang, R., Cotter, R. J., Reardon, I. M., Zurcher-Neely, H. A., Heinrikson, R. L., Ball, M. J. and Greenberg, B. D. 1993, J. Biol. Chem., 268, 3072.

53. Weinreb, P. H., Jarrett, J. T. and Lansbury Jr., P. T. 1994, J. Am. Chem. Soc., 116, 10835.
54. Raskatov, J. A. and Teplow, D. B. 2017, Scientific Reports, 7, 1.
55. Sugiki, T. and Utsunomiya-Tate, N. 2013, Biochem. Biophys. Res. Commun., 441, 493.
56. Sakai-Kato, K., Naito, M. and Utsunomiya-Tate, N. 2007, Biochem. Biophys. Res. Commun., 364, 464.
57. Murakami, K., Uno, M., Masuda, Y., Shimizu, T., Shirasawa, T. and Irie, K. 2008, Biochem. Biophys. Res. Commun., 366, 745.